2-28-2023

A fetal tumor suppressor axis abrogates MLL-fusion-driven acute myeloid leukemia

Mohamed Eldeeb

Ouyang Yuan

Nicola Guzzi

Phuong Cao Thi Ngoc

Anna Konturek-Ciesla

See next page for additional authors

Authors

Mohamed Eldeeb, Ouyang Yuan, Nicola Guzzi, Phuong Cao Thi Ngoc, Anna Konturek-Ciesla, Trine A Kristiansen, Sowndarya Muthukumar, Jeffrey Magee, Cristian Bellodi, Joan Yuan, and David Bryder

Cell Reports

Article

A fetal tumor suppressor axis abrogates MLL-fusion-driven acute myeloid leukemia

Graphical abstract

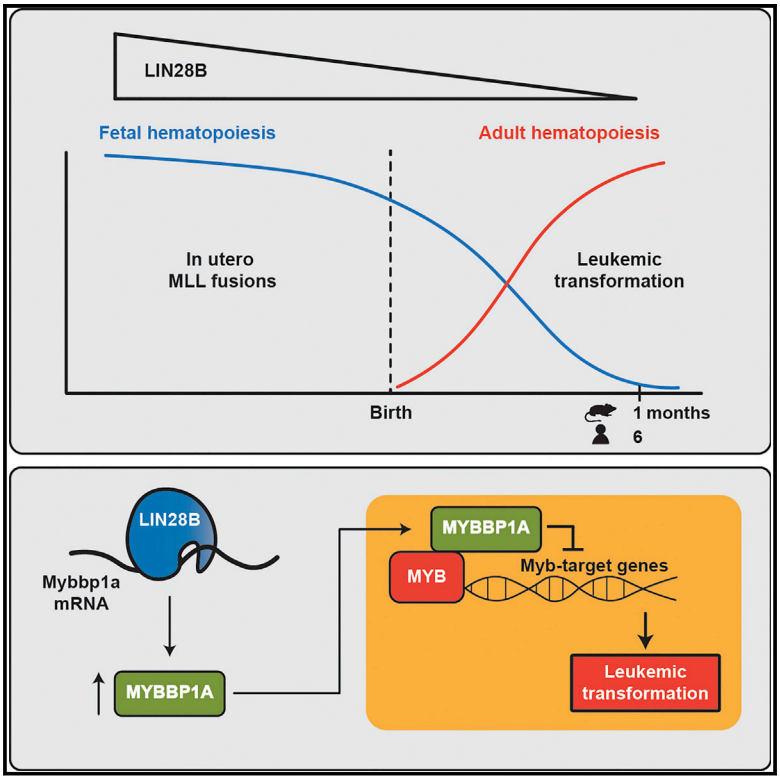

Highlights

- LIN28B does not become re-activated in human or murine AML
- The expression of LIN28B suppresses MLL-ENL-driven AML
- LIN28B compromises leukemic development by suppressing MYB activity
- The tumor-suppressor effects of LIN28B are largely driven by MYBBP1A

Authors

Mohamed Eldeeb, Ouyang Yuan, Nicola Guzzi, ..., Cristian Bellodi, Joan Yuan, David Bryder

Correspondence

david.bryder@med.lu.se

In brief

Eldeeb et al. report an LIN28B-mediated molecular layer of protection against perinatal AML. LIN28B expression associates with attenuated MYB activity driven by positive regulation of MYBBP1A. These insights into the roles of LIN28B can be exploited for therapeutic benefits.

Eldeeb et al., 2023, Cell Reports *42*, 112099
February 28, 2023
https://doi.org/10.1016/j.celrep.2023.112099

CellPress

Cell Reports

CellPress
OPEN ACCESS

Article

A fetal tumor suppressor axis abrogates MLL-fusion-driven acute myeloid leukemia

Mohamed Eldeeb,[1] Ouyang Yuan,[1] Nicola Guzzi,[1] Phuong Cao Thi Ngoc,[1] Anna Konturek-Ciesla,[1] Trine A. Kristiansen,[1] Sowndarya Muthukumar,[1] Jeffrey Magee,[2] Cristian Bellodi,[1] Joan Yuan,[1] and David Bryder[1,3,*]

[1]Division of Molecular Hematology, Department of Laboratory Medicine, Lund Stem Cell Center, Faculty of Medical, Lund University, 221 84 Lund, Sweden

[2]Division of Hematology and Oncology, Department of Pediatrics, Washington University School of Medicine, 660 S. Euclid Avenue, St. Louis, MO 63110, USA

[3]Lead contact

*Correspondence: david.bryder@med.lu.se

https://doi.org/10.1016/j.celrep.2023.112099

SUMMARY

MLL-rearrangements (MLL-r) are recurrent genetic events in acute myeloid leukemia (AML) and frequently associate with poor prognosis. In infants, MLL-r can be sufficient to drive transformation. However, despite the prenatal origin of MLL-r in these patients, congenital leukemia is very rare with transformation usually occurring postnatally. The influence of prenatal signals on leukemogenesis, such as those mediated by the fetal-specific protein LIN28B, remains controversial. Here, using a dual-transgenic mouse model that co-expresses MLL-ENL and LIN28B, we investigate the impact of LIN28B on AML. LIN28B impedes the progression of MLL-r AML through compromised leukemia-initiating cell activity and suppression of MYB signaling. Mechanistically, LIN28B directly binds to MYBBP1A mRNA, resulting in elevated protein levels of this MYB co-repressor. Functionally, overexpression of MYBBP1A phenocopies the tumor-suppressor effects of LIN28B, while its perturbation omits it. Thereby, we propose that developmentally restricted expression of LIN28B provides a layer of protection against MYB-dependent AML.

INTRODUCTION

Acute myeloid leukemia (AML) is the most common subtype of acute leukemia in adults, with increased predisposition coupled to advancing age. In children, while acute lymphoblastic leukemia is the most prevalent subtype, AML still constitutes ~20% of these cases, with approximately one-third of children not reaching 5-year survival.[1]

AML arises in a single immature hematopoietic cell upon acquisition of genetic events that lead to the formation of leukemia initiating cells (LICs). LICs reside at the apex of the AML hierarchy, and maintain disease progression through their high self-renewal potential and compromised differentiation.[2] The prognosis associated with AML varies substantially, with the heterogeneity of the disease with regard to immunophenotype, cytogenetic, and molecular aberrancies rendering some subtypes more aggressive. Chromosomal translocations that involve the Mixed-lineage leukemia 1 (*MLL1/KMT2A*) gene generate some of the most aggressive forms of AML, with an incidence of MLL-rearrangements (MLL-r) in ~15%–20% of pediatric and ~10% of adult AML cases.[3,4]

Despite similarities, AML in children and adults can be viewed as two separate diseases.[1,5] While secondary mutations drive AML leukemogenesis, pediatric AML samples have one of the lowest mutational rates among all cancers, which has challenged the generality of a two-step model of AML transformation.[1,5] Furthermore, myeloid-lineage bias, genome instability, clonal hematopoiesis, and myelodysplasia, are all well-known predisposing factors exclusive to adult AML.[5,6] Accumulating evidence also supports a prenatal origin of many driver mutations in pediatric AML, yet overt transformation usually occurs postnatally.[7–10] How fetal hematopoiesis and growth signals contribute to the disease patterns in pediatric leukemogenesis remains largely underexplored.

LIN28B is a highly conserved RNA-binding protein whose expression is mostly restricted to embryonic development, with a well-established role as a regulator of fetal hematopoiesis.[11,12] While the best studied mechanism of LIN28B in hematopoiesis is its ability to negatively regulate *let-7* microRNA (miR) biogenesis, leading to de-repression of transcripts under *let-7* miR control,[11,13–15] LIN28B can also modulate translation by direct binding to mRNAs.[16–19] Several studies have highlighted the oncogenic properties of LIN28B in various cancer contexts.[20] However, in MLL-r AML, the role of LIN28B has been a subject of debate, with some studies suggesting an oncogenic role,[21–23] and others proposing tumor-suppressor activities of LIN28 [24,25].

Here, using a dual-transgenic system for MLL-ENL and LIN28B, we observed an inverse correlation between LIN28B activity and AML progression. We found that LIN28B compromised the LIC activity of both preleukemic and leukemic MLL-r AML, which was underwritten by a suppression of MYB activity.

Mechanistically, LIN28B bound directly to MYBBP1A mRNA, which associated with enhanced protein levels of this negative regulator of MYB. Thus, by providing details on the tumor-suppressive roles of a fetal molecular pathway, our work contributes to an increased understanding of the distinct patterns of pediatric AML development and that can potentially be harnessed for therapeutic benefit.

RESULTS

LIN28B expression is low in pediatric and adult human AML

We initially investigated expression of *LIN28B* mRNA in cohorts of adult (n = 579) and pediatric (n = 45) human AML. Samples were obtained from the Cancer Genome Atlas (TCGA) database and included several MLL-rearranged samples (18 and 10 of the adult and pediatric samples, respectively).[26,27] Both cohorts presented with clear expression, although somewhat variable, of the prominent AML-associated genes *HOXA9*, *MYC*, *MYB,* and *CEBPA* (Figures 1A and 1B). By contrast, expression of *LIN28B* was absent in most samples (474 of 484, 97.9%) and in the few cases that it was present (10 of 484, ~2%), it was very low (Figures 1A and 1B). Additional data from the BEAT and LECEGENE cohorts,[27–31] as well as interrogations of a panel of 40 human AML cell lines revealed similar results. From these data, we concluded that expression of the fetal regulator LIN28B does not typically associate with either adult or pediatric human AML, including MLL-r subtypes.

Lin28b is not induced by an MLL-ENL fusion oncogene

The results on *LIN28B* expression in human AML (Figures 1A and 1B) contradicted those from a few previous studies, in which *LIN28B* expression associated with poor AML prognosis and enhanced leukemia aggressiveness.[21–23] As MLL-fusions in general associate with poor AML prognosis,[3] we interrogated the link between MLL-fusion expression and LIN28B expression further by evaluating the expression of *Lin28b* upon induction of an MLL-ENL (ME) fusion oncogene. For this, we used a transgenic mouse model (iME) in which ME can be induced by doxycycline (DOX).[32] We isolated $Lin^{-}Sca^{+}Kit^{+}CD150^{-}CD48^{+}$ (granulocyte/monocyte/lymphoid progenitors, hereafter referred to as GMLPs/LICs) from iME mice, cultured cells for 3 days in the presence of DOX, which was followed by cDNA isolation and quantitative reverse-transcription PCR (qRT-PCR). This revealed that ME failed to induce *Lin28b* expression (Figure 1C).

Downregulation of *miR-150* has been shown essential for MLL-r driven AML, as it targets critical genes such as *MYB*, and MLL-fusion expression was previously suggested to alleviate *miR-150* expression through the induction of *MYC* and *LIN28*.[21] This was proposed to induce an auto-regulatory leukemogenic circuit whereby elevated *FLT3* and *MYB* expression led to further induction of *HOXA9*, *MEIS1*, *MYC,* and *LIN28B*.[21] In other work, downregulation of *let-7* miR family members, which are direct targets of LIN28B,[13] has been proposed to underlie enhanced proliferation and leukemogenesis of AML cells.[21–23] The links between LIN28B and miR regulation led us to explore a potential connection between MLL-fusion and miR expression. miR sequencing of iME cells revealed that *miR-150* was among the top downregulated miRNAs upon ME induction (Figure S1A andFigure 1D), along with pronounced downregulation of *miR-342* and *miR-146a*, which represents two other miRs downregulated in AML[33] (Figure 1D and Table S1). Conversely, miRs previously shown to associate with higher expression in AML, including *miR-196b* and *miR-155*,[33] were strongly induced by ME (Figure 1D). As for miRs of the let-7 family, we observed clear expression of *let-7b* and *let-7c* upon ME induction (log2FC 1.3, Figures 1D and S1A), while other *let-7* members were less affected (Table S1).

Taken together, our miR profiling corroborated previous observations on miRs induced and repressed in AML, including for selected miRs of the *let-7* family. However, our findings that LIN28B was rarely associated with either human or preleukemic murine AML indicated, in contrast to previous suggestions,[21–23] less evidence for involvement of LIN28B in these processes.

Enforced LIN28B expression corrupts ME-mediated AML initiation

MLL-fusions can arise in utero,[7,8,10] which coincides with the developmentally restricted expression of LIN28B (Figure S1B). In light of this, and the discrepancy between previous reported results and ours regarding LIN28B expression levels in human and murine AML (Figure 1), we interrogated the role of LIN28B in MLL-r AML. For this, we crossed the iME strain[32] to mice with a DOX-inducible LIN28B transgene[34] (Figure 2A). Thereby, we obtained primary cells that expressed only the MLL-ENL fusion (referred to as ME), or that expressed LIN28B together with ME (referred to as L28BME) following provision of DOX. The expression of the inducible genes, *ME* and *LIN28B*, and their functionally relevant target genes *Hoxa9* and *Hmga2*, respectively, was confirmed by qRT-PCR (Figures 2B and S2A), with *Lin28b* levels of similar magnitude as those in hematopoietic progenitors from fetal liver (Figure S1B).

To investigate the consequence of LIN28B expression on ME leukemia development, we competitively transplanted 1,000 GMLPs, isolated from either ME or L28BME mice (all dual-expressing CD45.1/2), into separate groups of lethally irradiated CD45.2 C57BL/6 recipients. As reported,[32] all mice receiving ME cells developed leukemia within 3–6 months (Figure 2C). By contrast, we observed a decrease in incidence and an increase in AML latency upon co-expression of LIN28B (Figure 2C), translating into a complete abrogation of AML in ~60% of L28BME mice (Figure 2C). FACS analysis of peripheral blood (PB) cells 4 weeks after transplantation revealed multilineage contribution from both ME and L28BME cells (Figure S2B), while PB analyses of healthy L28BME mice at the experimental endpoint confirmed the presence of donor derived cells, but these were now almost exclusively $CD19^{+}B220^{+}$ B cells (Figure S2C). Most importantly, qRT-PCR analysis on L28BME cells from mice succumbing to disease revealed a striking reduction/lack of *LIN28B* expression levels and its target gene *Hmga2*. This contrasted clear expression of *ME* and *Hoxa9* in the same samples (Figure 2D), demonstrating that in the instances when leukemic development was observed from L28BME cells, the *LIN28B* transgene (and its target *Hmga2*) had become silenced.

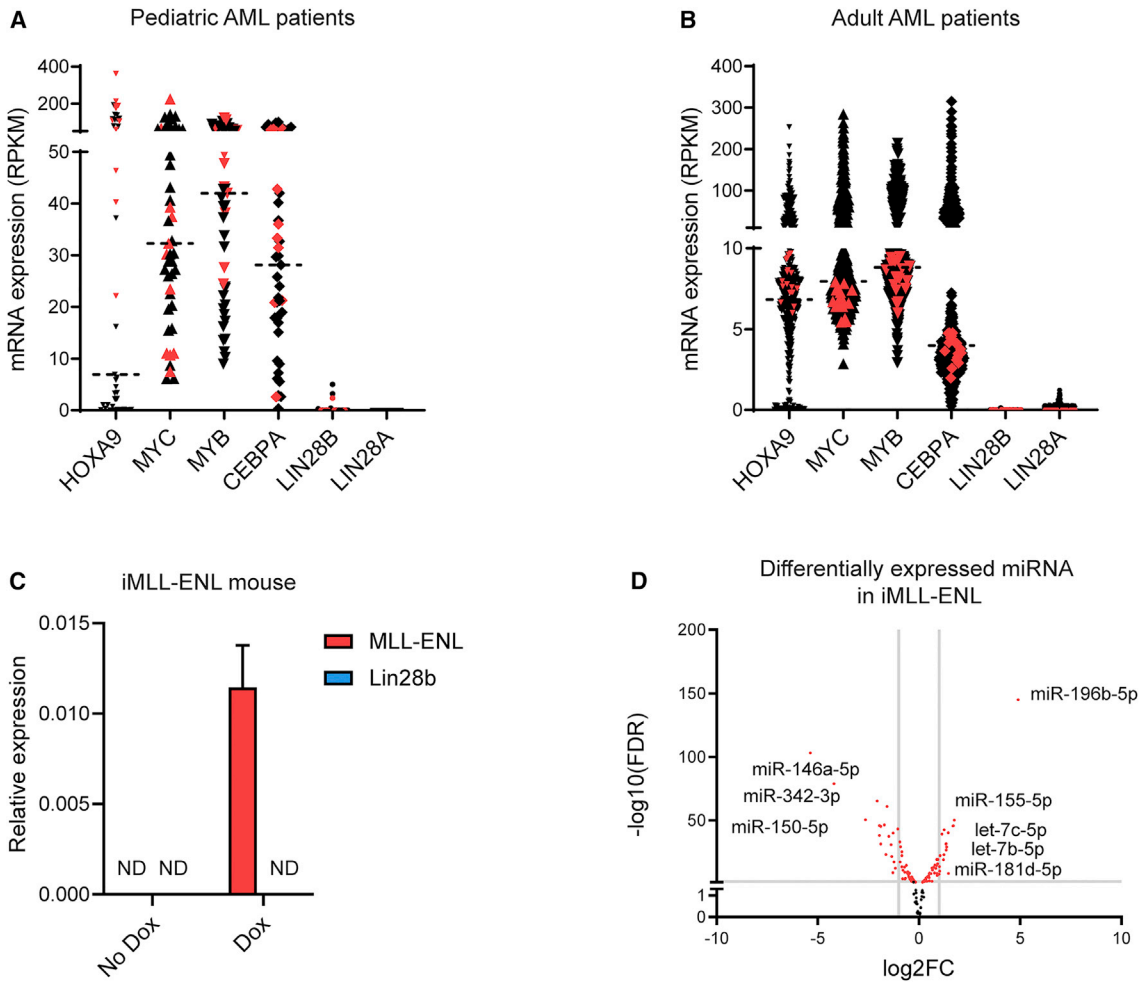

Figure 1. LIN28B and candidate miR expression in AML

(A and B) mRNA expression levels of prominent leukemia-associated genes in AML in comparison to *LIN28B* expression in (A) pediatric (n = 45) or (B) adult AML patient (n = 579) cohorts. Individual samples are displayed with MLL-r samples marked in red. Dashed lines represent median.

(C) Expression levels of *LIN28B* and *ME* in GMLPs isolated from iMLL-ENL mice in the absence (no DOX) or presence (DOX) of ME expression. ND = not detected. Bars indicate mean values, and error bars represent SEM.

(D) Volcano plot showing the top differentially expressed miRNAs (red) upon ME induction. miRs with a minimum expression of 100 TMM in one group were selected, and their corresponding log2FC and FDR values were plotted. Vertical lines indicate log2FC of −1 and +1 and the horizontal line a –log10 (FDR) of 2, with n = 4 replicates/group.

See also Figure S1 and Table S1.

Enforced expression of LIN28B potently abrogates RAS-mediated AML transformation

In vivo leukemia development in the iME model depends on the acquisition of relevant second hits.[35] Activating mutations in the RAS pathway are the most common secondary mutations found in MLL-rearranged leukemias, and are sufficient for MLL-r AML transformation also in the mouse.[36] Therefore, to study the influence of LIN28B expression on this more aggressive AML, as opposed to its influence on more spontaneous leukemia initiation (Figure 2C), we transduced GMLPs from ME and L28BME mice with an HRAS Q61L retrovirus. Transplantation of these cells led to rapid leukemia development/mortality in the ME group (Figure 2E). By contrast, in the group receiving L28BME cells, we observed a dramatically reduced disease incidence (Figure 2E). Noteworthy, in the only case in which an L28BME + HRAS Q61L recipient succumbed to disease, it presented as a T-ALL (T cell acute lymphoblastic leukemia) rather than AML (Figure S2D).

In vitro propagation of candidate ME leukemia-initiating cells is compromised by LIN28B

To assess the intrinsic effects of LIN28B on ME activity, we next evaluated the *in vitro* proliferative capacity of ME and L28BME LICs by culturing preleukemic GMLPs. The proliferative activity was first evaluated after 6 days of culture, at which time no difference in proliferation could be observed as a consequence of LIN28B expression (Figure S2E). However, when cells were subjected to serial replating, a pronounced

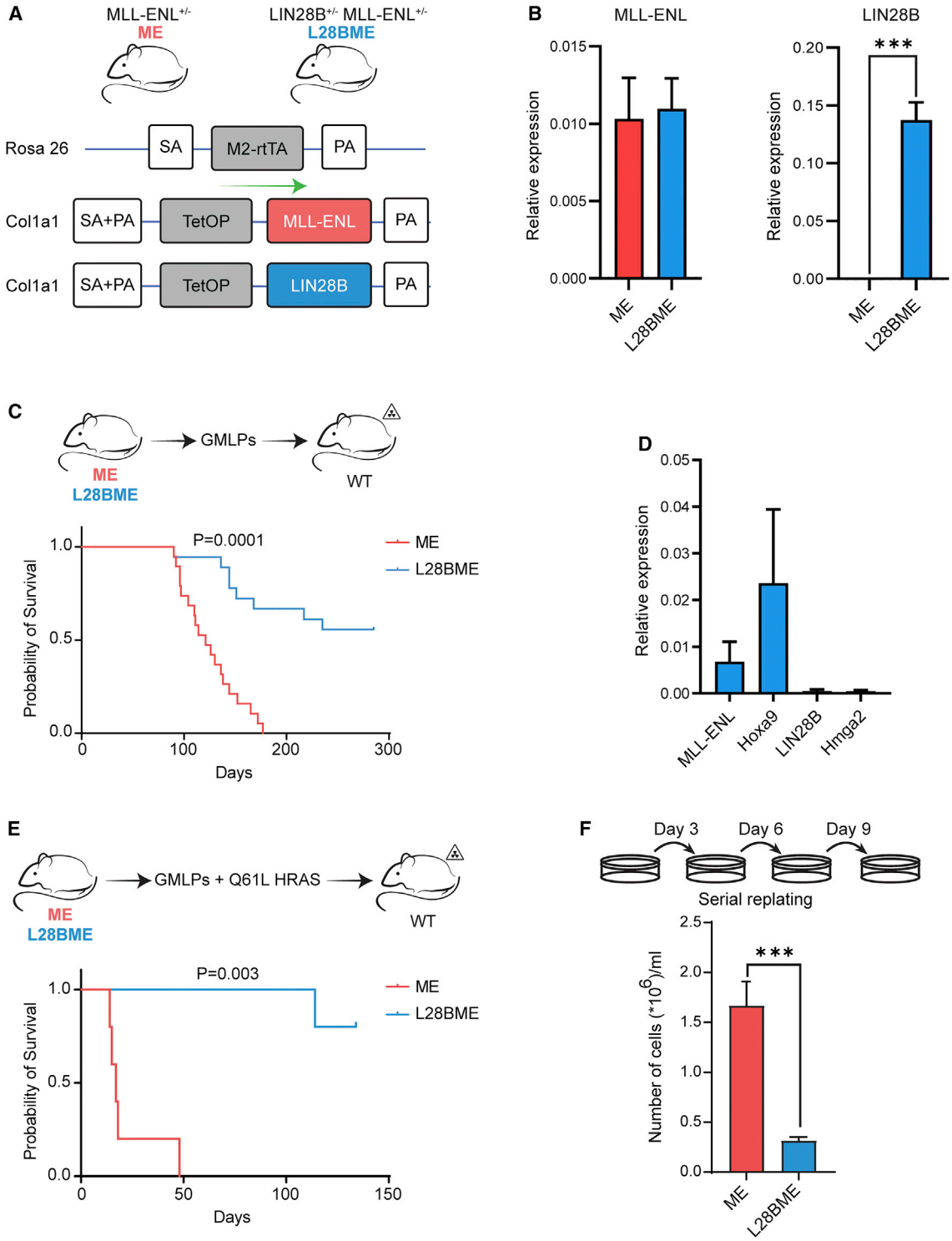

Figure 2. LIN28B interferes with AML development and propagation

(A) Schematic description of the mouse models used.

(B) qRT-PCR was performed on GMLPs from mice with indicated genotypes, confirming the expression of *ME* and *LIN28B* following DOX-mediated transgene induction. n = 5 replicates/group.

(C) Experimental outline of transplantation experiments of LICs to assess the impact of LIN28B expression on leukemia development (top), and Kaplan-Meier survival curves of the transplanted mice (bottom). n = 20 mice per group. Log rank (Mantel-Cox) test was used.

(legend continued on next page)

decrease in L28BME cell numbers was observed (Figure 2F). These data suggested that the impaired capacity of LIN28B to propagate ME-expressing (pre)leukemic cells is a direct effect on LICs.

Molecular profiling reveals that LIN28B dysregulates *Let-7* miRs and associates with diminished AML and c-MYB signatures

During fetal development, LIN28B expression is a major driver of lymphopoiesis and its enforced expression in adult hematopoietic stem/progenitor cells is sufficient to instate a fetal-like lymphoid program.[11] This is, at least in part, mediated through the ability of LIN28B to suppress *let-7* biogenesis.[14] We hypothesized that the mechanisms whereby LIN28B compromises AML initiation and propagation from ME-LICs could be reflected in their transcriptomes, which we explored by miR sequencing (miR-seq) and RNA sequencing (RNA-seq).

In line with the notion that *let-7* miRs are the major miR targets of LIN28,[13] we observed their strong downregulation in L28BME cells (Figure 3A and Table S2). By contrast, we failed to observe changes in miR targets previously shown to be essential in MLL-leukemogenesis, such as *miR-150* and *miR-196b* (Figure S3A and Table S2).

Approaching mRNA expression changes, we observed reassuringly that Lin28b was the highest differentially upregulated gene in L28BME cells. This was accompanied by prominent upregulation of many fetal and/or lymphoid-associated genes, including for instance *Igf2bp3*, *Hmga2*, *Arid3a*, *Arid3b*, *Rag1,* and *Rag2* (Figure 3B and Table S3). Several of these genes are targets of *let-7*,[18] which was further confirmed by applying an miR-prediction tool on the most upregulated genes in L28BME cells (Figure 3C).

For genes downregulated upon enforced LIN28B expression, perhaps the clearest observation was reduced expression of stem- and early myeloid-associated genes (Figure 3B and Table S3). To further validate this, we applied the CellRadar tool (https://karlssong.github.io/cellradar/). CellRadar uses publicly available data on lineage-associated genes to identify cell type enrichments from a list of genes. Again, this revealed that L28BME cells, in contrast to ME cells, associated with reduced transcript levels linked to stem/myeloid progenitors and an enrichment of lymphoid-associated transcripts (Figure 3D).

To further mine the mRNA expression data, we applied gene set enrichment analysis (GSEA).[37,38] This revealed that L28BME cells associated with a depletion of MLL-fusion leukemia signatures[39,40] and an AML leukemia stem cell (LSC) signature[41] (Figure 3E, upper panel). This was accompanied by an enrichment for fetal-lymphoid differentiation and an apoptosis signature (Figure 3E, lower panel).[42,43] Finally, we observed repression of c-MYB target genes in L28BME cells[44] (Figures 3E and S3B). This was of particular interest because MYB has been previously shown to critically govern MLL-r AML development, with its partial or transient suppression completely eradicating MLL-fusion leukemia.[44]

The tumor-suppressor activity of LIN28B is independent of *Let-7* repression

Given the observed repression of c-MYB targets in L28BME cells (Figure 3), we sought to interrogate the mechanisms whereby LIN28B mediates this effect. LIN28B acts either via repression of *let-7* biogenesis, or via direct binding to individual mRNA targets to subsequently enhance or repress their translation (Figure 4A).[16–19]

We began by investigating the potential role of *let-7* repression in AML. For this, we introduced an *let-7* sponge (or an empty vector as control) that targets the entire family of *let-7* miRs to ME-LICs[45] (Figure 4B). To accelerate disease development, cells from both groups were in addition co-transduced with an R295C mutant version of Moesin (MSN), which dramatically accelerates murine MLL-ENL-mediated AML progression.[35] Double-transduced cells were transplanted, and recipients were monitored for disease development. We observed only a slight delay in disease development in the *let-7* sponge group that failed to reach significance (Figure 4B). These results suggested that repression of the canonical *let-7* pathway is not the primary mechanism whereby LIN28B mediates its tumor-suppressor activities, and instead entertained that this activity is mediated by the mRNA binding capacity of LIN28B.

Mybbp1a is a direct target of enforced LIN28B expression

To map the transcriptome-wide LIN28B-RNA associations in an unbiased manner, we began by performing individual-nucleotide resolution UV cross-linking and immunoprecipitation followed by sequencing (iCLIP-seq)[46] on L28BME GMLPs (Figure 4C), with ME cells used as a control for nonspecific binding (Figure 4D).

In agreement with previous studies,[16,19] the obtained reads associated with an enrichment of the LIN28B consensus binding motif (GGAG) (Figure 4E). Investigating the obtained reads more broadly revealed a particular enrichment for mRNAs (3′ UTR and CDS regions), and only a minor association with 5′ UTR and mature miR binding (Figure 4F and Table S4), which is also in line with previous CLIP studies on LIN28.[17] One of these bound mRNAs, *Mybbp1a*, presented with several LIN28B-binding peaks in the coding and non-coding regions of its mature/spliced mRNA (Figure S4A). This was of immediate interest to us given the previously reported ability of MYBBP1A to repress c-MYB,[47,48] as well as the high protein levels of MYBBP1A in

(D) qRT-PCR on leukemic BM (bone marrow) cells from diseased L28BME mice, demonstrating that leukemias have lost expression of the LIN28B transgene. n = 3.

(E) Experimental outline to determine the impact of LIN28B on ME+ active RAS-driven AML (top), and Kaplan-Meier survival curves of transplanted mice (bottom). n = 5 mice per group. Log rank (Mantel-Cox) test was used.

(F) LIN28B compromises the *in vitro* serial replating ability of candidate LICs. A total of 10,000K GMLPs/condition were sorted, cultured, serially replated (1/10 of the well at each split), and counted on day 12. n = 3 replicates/group. Bars indicate mean values, and error bars represent SEM. *p < 0.05, **p < 0.01, ***p < 0.001; n.s., not significant. Student's t test was used, unless otherwise stated.

See also Figure S2.

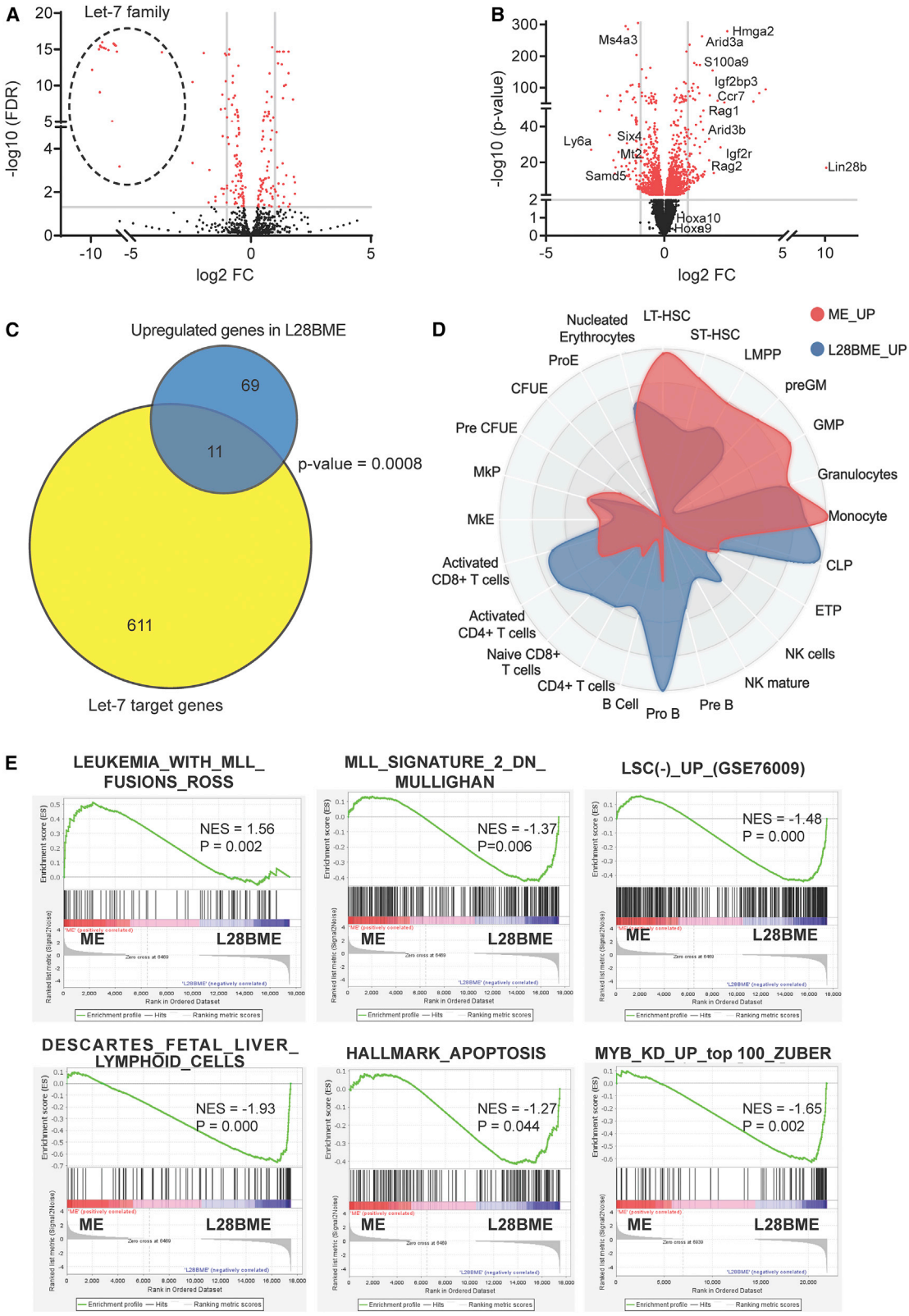

(legend on next page)

fetal hematopoietic progenitors in comparison with adults.[49,50] To confirm these findings, we performed RNA Immunoprecipitation (RIP)-qPCR from L28BME cells against *Mybbp1a* (Figure 4G) and a few other selected targets from our iCLIP-seq data (Figure S4B). This verified direct associations between LIN28B and these mRNAs (Figure S4B).

Although context-dependent, MYBBP1A has been previously described to have tumor-suppressor activities, with protein levels inversely correlating with c-MYB activity.[48] To determine the impact of the LIN28B-*Mybbp1a* mRNA interaction on MYBBP1A protein levels, we performed western blot on protein lysates from ME or L28BME cells. This revealed a striking increase in MYBBP1A in the LIN28B-expressing cells (Figure 4H), which could not be deduced from the mRNA transcript levels (Figure 4I).

Taken together, these experiments suggested that the tumor-suppressor activities of LIN28B are mediated by its capacity to bind distinct mRNAs and alter their translation, with the binding to Mybbp1a mRNA emerging as a direct candidate target for such a mechanism.

Enforced expression of MYBBP1A represses murine and human MLL-r AML

With MYBBP1A as a candidate mediator for the tumor suppressor activity of LIN28B, we decided to directly investigate its influence on ME-driven AML. For this, we retrovirally transduced ME-LICs with an MYBBP1A overexpression vector, or with an empty vector (EV) as a control. As expected, we observed an increase in *Mybbp1a* mRNA levels following MYBBP1A overexpression (Figure 5A). However, this was not accompanied by a rise in MYBBP1A protein levels (Figure 5B, left lane), which suggested post-translational regulation/degradation of MYBBP1A.

Under normoxic conditions, Proline 693 of MYBBP1A can become ubiquitinylated by von Hippel-Lindau (VHL), which leads to MYBBP1A protein degradation.[51] With this additional layer of regulation of MYBBP1A, we interrogated whether blocking proteasomal degradation would be sufficient to equalize MYBBP1A levels in ME and L28BME. For this, we treated Kit^+ cells from ME and L28BME with the proteasome inhibitor MG132 for 4 h and then measured MYBBP1A levels. MG132 treatment allowed for the detection of MYBBP1A in ME cells; however, to a much lower extent in comparison to MYBBP1A levels in L28BME cells (Figure S4C). This suggested that the LIN28B-mediated enhancement of MYBBP1A is not only the result of lack of proteasomal degradation, but also due to an overall increase in MYBBP1A translation.

Although in a different cellular context, substitution of Proline 693 with Alanine was shown to be sufficient to prevent this degradation.[51] Therefore, we transduced ME-LICs with MYBBP1A A693 rather than wild-type (WT) MYBBP1A. Indeed, overexpression of MYBBP1A A693 led to a pronounced increase in MYBBP1A protein levels in ME-LICs (Figure 5B). With a way to enforce expression of MYBBP1A protein, we first evaluated its impact on ME-LIC differentiation *in vitro*. This revealed an increase in the frequency of granulocytes/terminally differentiated myeloid cells following introduction of MYBBP1A A693 (Figure 5C), in line with previous studies showing an increase in granulocytic differentiation following loss of c-Myb.[52]

To explore the impact of enforced expression of MYBBP1A on human MLL-r driven AML, we transduced THP-1 cells, a human cell line for infant MLL-AF9-driven AML, with MYBBP1A A693 or EV as a control. Equal numbers of transduced cells were sorted from each condition and maintained in culture for 20 days. This revealed a dramatically reduced proliferation of MYBBP1A A693 transduced THP-1 cells (Figure 5D).

Next, we explored the consequences of MYBBP1A overexpression on ME leukemia initiation *in vivo*. We transplanted 5,000 ME-LICs transduced with MYBBP1A A693 (or EV) into lethally irradiated recipients (Figure 5E), which revealed a significant delay in leukemia incidence in the MYBBP1A A693 group (Figure 5E).

Thus far, both our *in vitro* and *in vivo* experiments had indicated compromised ME-LIC activity upon MYBBP1A expression. To assess the magnitude of deterioration in LIC function further, we transplanted different doses of ME MSN R295C LICs with or without MYBBP1A A693 (Figure 5F). Despite the added aggressiveness of MSN R295C, all MYBBP1A A693 groups presented with higher overall survival compared with their EV counterparts (Figure 5F). Moreover, disease latencies of the 5,000 and 2,000 cell doses of MYBBP1A A693 corresponded to those of the 1,000 and 500 cell doses of EV, respectively (Figure 5F), suggesting ~5-fold reduced LIC activity in the MYBBP1A A693 group. The tumor-suppressor activity of MYBBP1A became more evident in the groups with lower cell doses, where leukemia penetrance dropped to 25% following enforced MYBBP1A A693 expression (Figure 5F).

Finally, we used a CRISPR-Cas9 gene editing system to investigate whether the knockout (KO) of *Mybbp1a* in L28BME could accelerate leukemia development.[53,54] Ribonucleoprotein (RNP) complexes of CAS9 and a mix of guide RNAs (gRNAs) against *Mybbp1a* were delivered to GMLPs from L28BME with an HRAS Q61L mutation. Sanger sequencing confirmed efficient deletion of *Mybbp1a*, with an editing efficiency of ~97% (Figures S5A and S5B). A total of 5,000 cells with WT *Mybbp1a* (control) or KO *Mybbp1a* were transplanted into lethally

Figure 3. LIN28B alters the ME-fusion associated miR and mRNA expression patterns

(A) Volcano plot showing the differentially expressed miRNAs (red) in L28BME GMLPs.

(B) Volcano plot highlighting the differentially expressed mRNA targets (red) in L28BME GMLPs. Gray lines in (A) and (B) represent log2FC of −1 and +1. n = 3 replicates/group.

(C) Overlap between the top predicted *let-7* targets (TargetScan, aggregate PCT >0.85) and upregulated genes in L28BME (log2FC > 1). Analyses were conducted using MIENTURNET (http://userver.bio.uniroma1.it/apps/mienturnet/).

(D) CellRadar analysis (https://karlssong.github.io/cellradar/) performed on the differentially expressed genes in each group, showing a reduced affiliation of stem cell-associated transcripts in L28BME cells along with an increase in lymphoid lineage affiliated genes.

(E) GSEA plots on ME and L28BME cells for selected AML-associated gene signatures. Determination of significance were made according to the guidelines of the respective analysis tools (see STAR Methods).

See also Figure S3 and Tables S2 and S3.

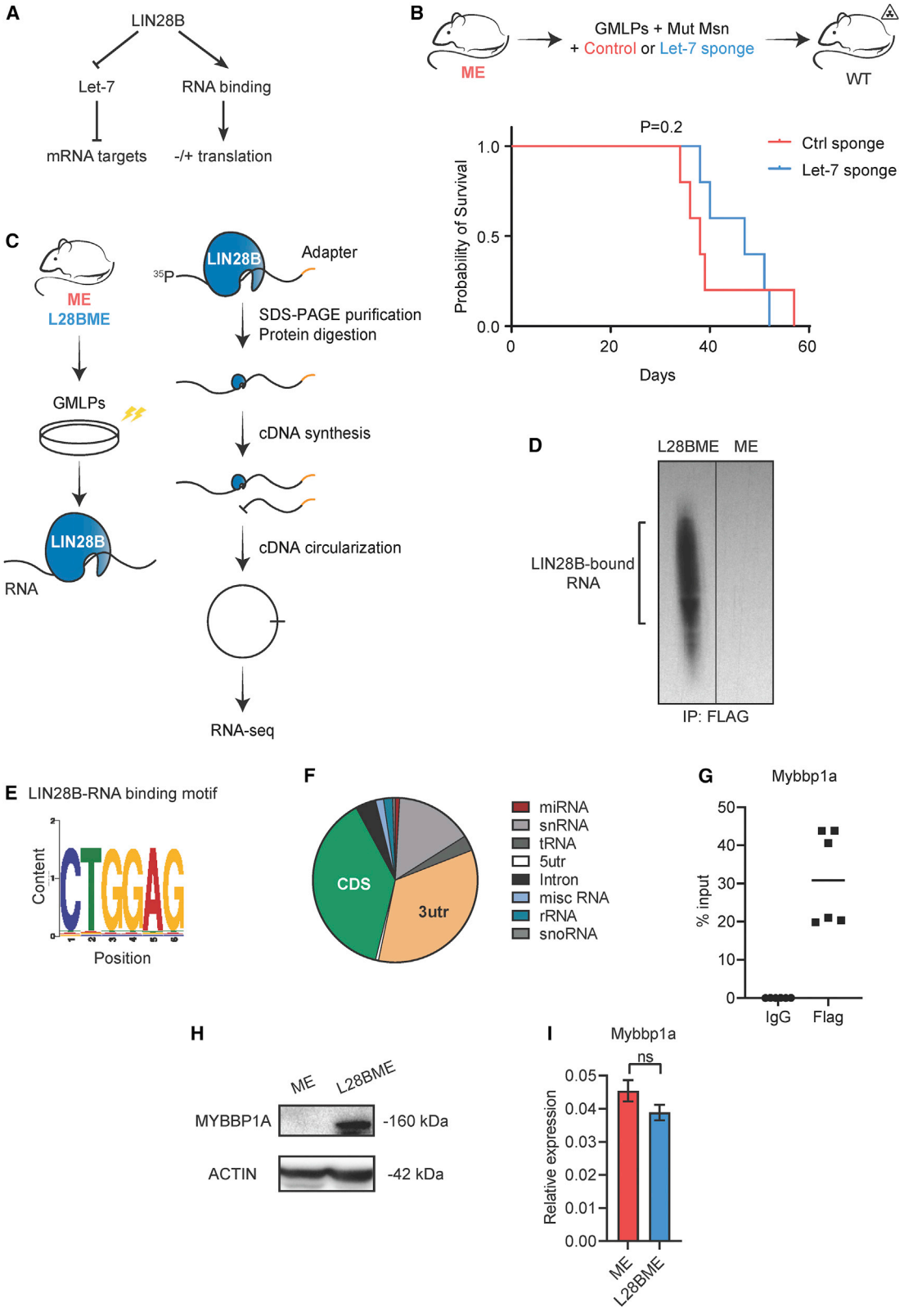

(legend on next page)

irradiated recipient mice and AML development was assessed. Indeed, KO of *Mybbp1a* associated with significant acceleration and penetration of AML (Figures 6B and S5C). Taken together, these data established that MYBBP1A expression interferes with ME leukemia initiation and development.

DISCUSSION

The molecular intricacies of pediatric MLL-leukemogenesis remain largely elusive. In this patient subgroup, MLL-fusions appear for the most part to arise in utero. In contrast to the situation in adults, pediatric MLL-fusion leukemias have been proposed to be sufficient to drive transformation, without the need for additional molecular lesions.[1,5,8,10] At the same time, the incidence of congenital/neonatal AML leukemia is very low.[9] Although it is well established that there exist distinct prenatal signals that promote organismal growth and cellular proliferation,[55] little is known about their relationship to oncogenesis.[56] Here, we tried to approach this issue by focusing on LIN28B, a master regulator of fetal hematopoiesis.[11,12]

Reactivation of LIN28 has been described in several human cancers, where LIN28 has been proposed as an oncogene.[20] In the context of leukemia, a few previous studies have proposed that LIN28 acts as a downstream target of MLL-rearrangements, where its expression associated with more aggressive disease.[21–23] In a diametrically opposing view, more recent studies have suggested that expression of LIN28 has a tumor-suppressor function in AML.[24,25] To reconcile some of these discrepancies, we began our work by interrogating an available cohort of AML patients.[1,27] This revealed that the vast majority of both pediatric and adult AML patient samples lack expression of *LIN28B* mRNA. Similarly, we failed to observe elevations of *Lin28b* mRNA levels in our inducible ME mouse model.

The role of Lin28 as a negative regulator of the *let-7* class of miRs is well established,[13] and we confirmed this in our ME model. However, we also observed that ME expression, in the absence of Lin28, can elevate the expression of some *let-7* miR family members. We interpret these results to be in line with the previously reported correlation between high *let-7* levels and worse prognosis in pediatric AML patients,[1] although *let-7* miRs might act as tumor suppressors in other cancer types.[13] Regardless, because we failed to observe any pronounced delays in leukemic development upon reducing *let-7* miRs, we rather entertain that the tumor-suppressor activity of LIN28B is largely *let-7* independent.

It has previously been established that enforced expression of LIN28B in adult hematopoietic stem/progenitor cells is sufficient to reestablish several aspects of fetal hematopoiesis.[11] Using our dual-transgenic mouse model, LIN28B potently impeded the development of ME-induced AML, with ~60% of the mice in the L28BME group failing to succumb to disease. Furthermore, when interrogating AML developing in this group, we failed to observe expression of LIN28B. While it remains unclear how the LIN28B transgene (but not ME) became silenced in these samples, these observations further strengthen the view that expression of LIN28B for the most part appears incompatible with ME-driven AML initiation. In addition, although co-expression of activating RAS mutations with MLL-fusions establishes very aggressive AML,[36] we found that the enforced expression of LIN28B in such settings also interferes with AML progression. Thus, LIN28B can in addition to interfering with spontaneous MLL-r AML formation also disrupt AML in settings involving relevant secondary driver mutations.

To identify downstream targets of LIN28B responsible for its tumor-suppressive activity, we initially subjected LICs to genome-wide expression profiling. This revealed a striking depletion of c-MYB target genes upon enforced expression of LIN28B, which was accompanied by significant decreases in MLL-leukemogenesis and LSC gene expression signatures and an enrichment for expression signatures associated with differentiation and apoptosis. Multiple studies have shown that MYB is an essential target of MLL-rearrangements, with critical roles for LSC maintenance.[44,57] This includes the ability of MLL-r to upregulate *Myb* levels by direct occupancy of the *Myb* promoter,[44] or indirectly through upregulation of *Hoxa9* and *Meis1* and repression of *miR-150*.[21] Intriguingly, all of these direct and indirect regulators of *Myb*, including for *Myb* itself, were found to be unaltered upon LIN28B expression. Thus, we sought for another mode of regulation.

Using protein-RNA-binding studies, we identified direct binding of LIN28B to *Mybbp1a* mRNA. Our choice to focus on *Mybbp1a* was primarily based on the original demonstration that MYBBP1A negatively regulates MYB activity.[47] MYBBP1A is critical for early embryonic development[49] and its protein levels in the hematopoietic system are higher in fetal as opposed to adult progenitors.[49,50] This is similar to the expression patterns of LIN28B. While not extensive, previous studies have demonstrated that MYBBP1A is degraded by VHL in a similar manner as the hypoxia inducible factor HIF-1a,[51] the latter of which can also act as a tumor suppressor in AML.[58] Regardless,

Figure 4. A direct interaction between LIN28B and Mybbp1a mRNA that associates positively with MYBBP1A protein levels

(A) Putative mechanisms whereby LIN28B has been shown to exert its gene regulatory activities.

(B) Experimental outline to assess the impact of *let-7* miRNAs inhibition on leukemia development (top), and Kaplan-Meier survival curves of the transplanted mice (bottom). n = 5 mice per group. Log rank (Mantel-Cox) test was used.

(C) iCLIP-seq strategy to identify genome-wide LIN28B-RNA interactions.

(D) Autoradiograph depicting the immunoprecipitated complexes of LIN28B-bound RNAs (lane 1) from L28BME and ME (nonspecific binding) cells (lane 2).

(E) Pie chart depicting the fractions of different RNA species bound to LIN28B in the iCLIP-seq experiment.

(F) The consensus LIN28B binding motif sequence extracted from the iCLIP binding peaks.

(G) RIP qPCR confirming direct binding of LIN28B to *Mybbp1a* mRNA.

(H) Western blot demonstrating exclusive expression of MYBBP1A following enforced expression of LIN28B.

(I) qRT-PCR demonstrating similar *Mybbp1a* mRNA levels in the presence or absence of LIN28B expression. n = 3 replicates/group. Bars indicate mean values, and error bars represent SEM. n.s., not significant. Student's t test was used.

See also Figure S4 and Table S4.

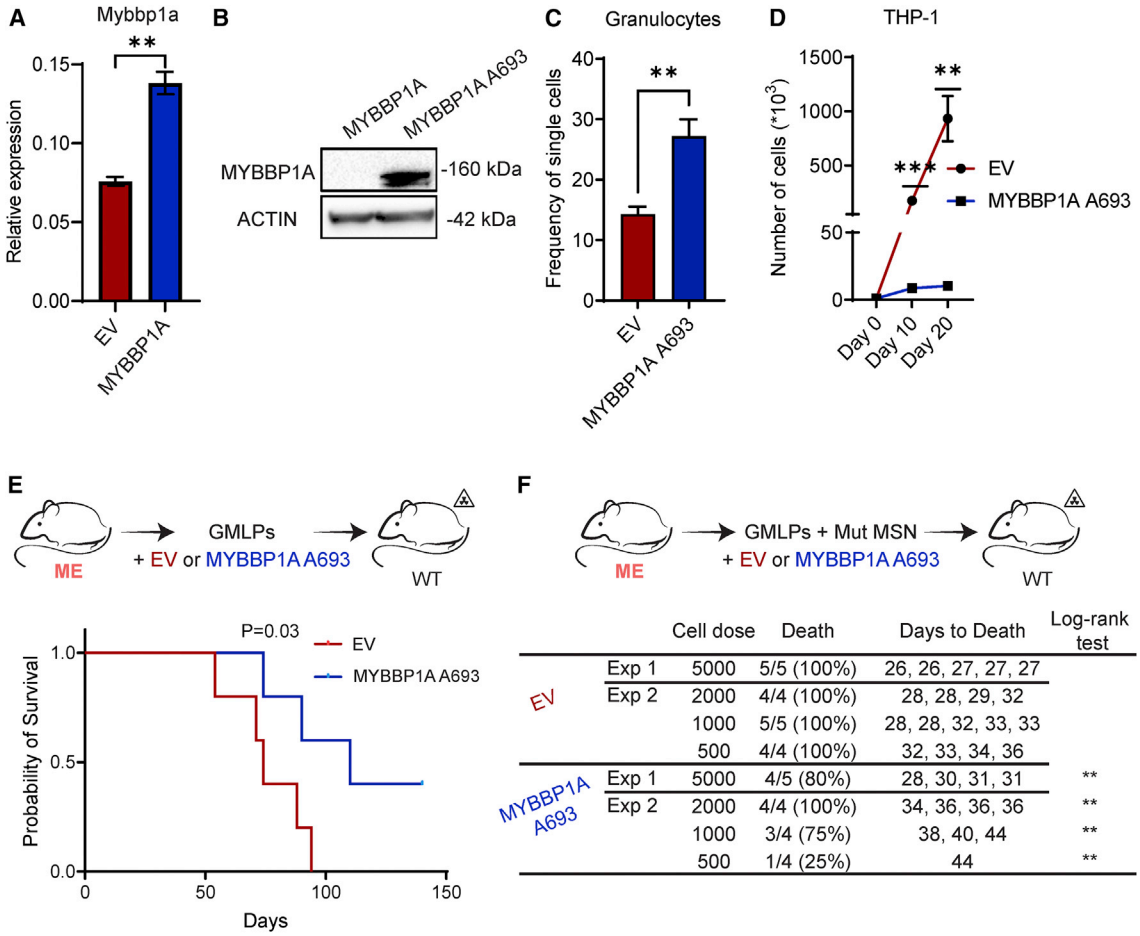

		Cell dose	Death	Days to Death	Log-rank test
EV	Exp 1	5000	5/5 (100%)	26, 26, 27, 27, 27	
	Exp 2	2000	4/4 (100%)	28, 28, 29, 32	
		1000	5/5 (100%)	28, 28, 32, 33, 33	
		500	4/4 (100%)	32, 33, 34, 36	
MYBBP1A A693	Exp 1	5000	4/5 (80%)	28, 30, 31, 31	**
	Exp 2	2000	4/4 (100%)	34, 36, 36, 36	**
		1000	3/4 (75%)	38, 40, 44	**
		500	1/4 (25%)	44	**

Figure 5. MYBBP1A corrupts ME leukemia initiation and propagation by impairing LIC activity

(A) qRT-PCR analysis of *Mybbp1a* following retroviral transduction of ME GMLPs with EV or MYBBP1A overexpression vector. n = 3 replicates/group.

(B) Western blot following enforced expression of WT or P693A mutant MYBBP1A.

(C) Enforced MYBBP1A A693 expression associates with enhanced preleukemic cell differentiation into granulocytes, which are defined by Ly6G and CD11b expression. n = 3 wells per condition.

(D) Cell counts of the AML human cell line THP-1 following transduction with EV or MYBBP1A A693 overexpression vector. n = 3 wells per condition.

(E) Experimental outline to determine the impact of MYBBP1A A693 expression on leukemia initiation (top), and Kaplan-Meier survival curves of transplanted mice (bottom). n = 5 mice per group.

(F) Experimental outline of LIC titration experiments to assess the impact of MYBBP1A on LIC function (top), with table of details and results (bottom). Log rank (Mantel-Cox) test was used in (E) and (F). Bars indicate mean values, and error bars represent SEM. *p < 0.05, **p < 0.01, ***p < 0.001; n.s., not significant. Student's t test was used, unless otherwise stated.

the hypoxia associating with the prenatal state provides one plausible mechanism for the higher expression of MYBBP1A during this period.[59] While MYBBP1A has not been extensively studied in the context of AML, its tumor-suppressive activities have been suggested in several other cancers, and where its lower levels associate with worse disease prognosis.[60] Mechanistically, loss of MYBBP1A has been reported to increase MYB activity and induce a metabolic shift toward oxidative phosphorylation; both of which have also been proposed to be critical for LIC maintenance.[60,61]

When overexpressed, we observed that MYBBP1A recapitulated several of the tumor-suppressor phenotypes of LIN28B in both murine and human cells. In addition, knockout of *Mybbp1a* in L28BME interfered with the tumor-suppressor activity of LIN28B. But how might LIN28B elicit enhanced MYBBP1A levels? While we can only speculate on this, it is well established that apart from the ability of LIN28B to negatively regulate miRs, LIN28B can also enhance translation of its mRNA binding partners by accompanying them to ribosomes and P-bodies,[62,63] and by recruitment of RNA helicase A to increase translation efficiency.[64] More recent structural studies have also suggested that LIN28 might reprogram translation by gaining access to dormant mRNPs via co-association to YB-1.[65] Thus, we propose that the direct binding of LIN28B to the mature form of Mybbp1a mRNA results in increased translation of MYBBP1A by any of these mechanisms. In addition, our demonstration that MYBBP1A is under proteasomal control suggests that higher MYBBP1A levels might also be the consequence of repressed proteasomal

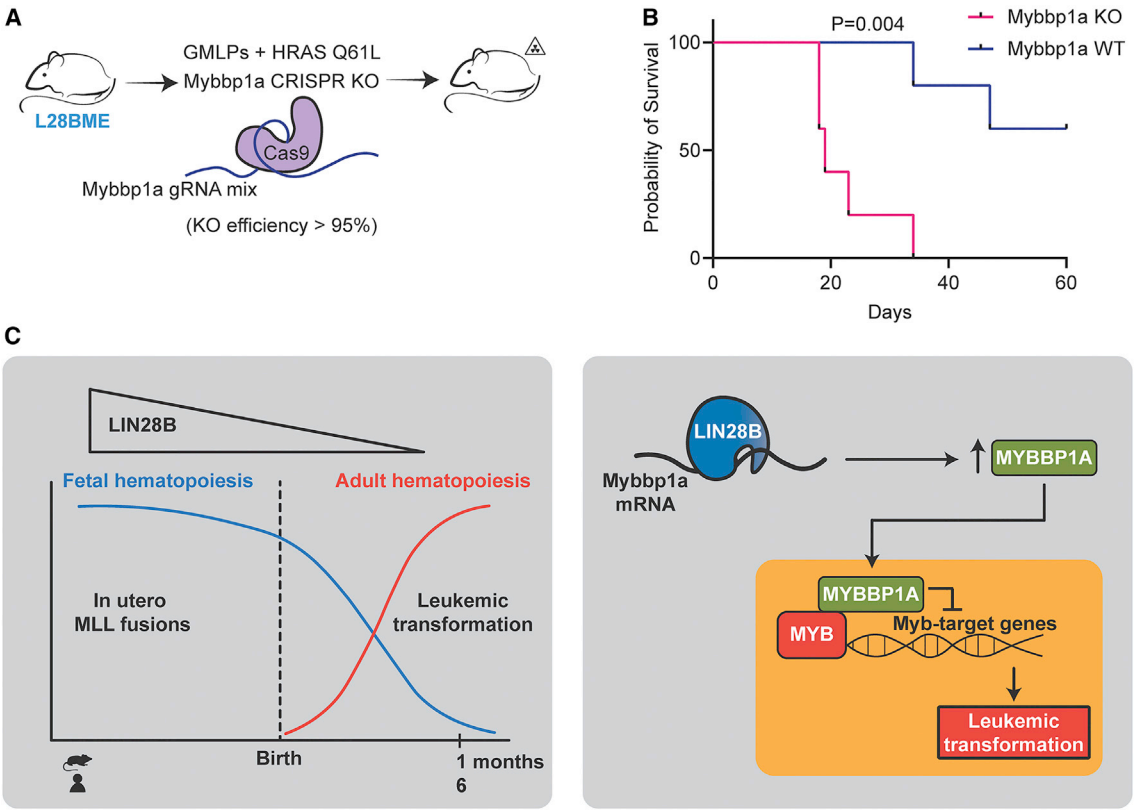

Figure 6. Knockout of Mybbp1a in L28BME interferes with the tumor-suppressor activity of LIN28B

(A) Experimental outline to determine AML development following *Mybbp1a* KO in L28BME LICs.

(B) Kaplan-Meier survival curves of recipient mice transplanted with L28BME LICs + HRAS Q61L and either *Mybbp1a* WT or KO. n = 5 mice per group. Log rank (Mantel-Cox) test was used.

(C) Model of the tumor-suppressor activity of LIN28B.

See also Figure S5.

degradation mediated by LIN28B, which was, however, insufficient to raise MYBBP1A to the levels observed following co-expression of LIN28B. Intriguingly, LIN28B was previously shown to coimmunoprecipitate with MYBBP1A in embryonic fibroblasts,[51] suggesting that these two proteins can also interact physically. Finally, since LIN28B is regarded as a master regulator of fetal hematopoiesis, where it exerts several functions and is part of multiple interactomes, our results do not exclude the existence of other LIN28B-mediated interactions that might synergistically contribute to its tumor-suppressor activities.

To conclude, our work illustrates an inverse correlation pattern between LIN28B expression and AML development, which given the specific ontogenic context of LIN28B should be of relevance to the paradigm of pediatric AML (Figure 6). We propose LIN28B → MYBBP1A –| MYB as a tumor suppressor axis that restricts MLL-r AML and perhaps also other AML subtypes with an MYB involvement. In this view, the developmentally restricted expression of LIN28B provides a natural protection against MYB-dependent tumors, while its abrupt decline a few weeks after birth presents an opportunity for oncogenesis (Figure 6). Whether and how this can be exploited also for therapeutic benefit across ages represents exciting avenues for future work.

Limitations of the study

Although we could narrow down the tumor-suppressor effects of LIN28B and showed that it is largely mediated through binding to MYBBP1A mRNA, the possibility of other targets that can synergistically contribute to AML suppression remains to be explored. In addition, while we focused on studying AML, little is known about how the expression of LIN28B might affect ALL, the most common leukemia in pediatrics. Further studies are needed to address these questions.

While we validated our findings in a human cell line for childhood leukemia, a direct clinical link is still lacking. This is challenging to establish since most patients are usually admitted to clinic at a relatively advanced disease stage, which makes it difficult to study the early steps of disease initiation. In addition, the critical stages of development at which both LIN28B expression and MLL-r coexists, and the natural decline of LIN28B shortly after birth, impose both technical and ethical challenges for obtaining primary patient material.

STAR★METHODS

Detailed methods are provided in the online version of this paper and include the following:

SUPPLEMENTAL INFORMATION

Supplemental information can be found online at https://doi.org/10.1016/j.celrep.2023.112099.

ACKNOWLEDGMENTS

We acknowledge Roberto Munita, Maciej Ciesla, Leal Oburoglu, Hugo Åkerstrand, and Pekka Jaako for valuable scientific discussions and technical support. Some of the results shown here are based on data generated by the TCGA Research Network: https://www.cancer.gov/tcga. J.M. is a Leukemia and Lymphoma Society scholar. The work was supported by grants from the Tobias Foundation, the Swedish Cancer Foundation, the Knut and Alice Wallenberg foundation, Swedish Childhood Cancer foundation and the Swedish Research Council. The authors declare no competing financial interests.

AUTHOR CONTRIBUTIONS

M.E. designed the research, performed experiments, analyzed data, and wrote the manuscript; O.Y. and S.M. performed experiments; N.G. and C.B. designed and performed the iCLIP-seq, and P.C.T.N. and A.K-C. performed the bioinformatic analysis; J.Y. provided access to the Lin28B-related reagents; J.M. provided key input and protocols for CAS9-RNP experiments; T.K., J.Y., and J.M. contributed to the discussion. D.B. supervised the project, was responsible for funding acquisition, designed the research, analyzed data, and wrote the manuscript.

DECLARATION OF INTERESTS

The authors declare no competing interests.

INCLUSION AND DIVERSITY

We support inclusive, diverse, and equitable conduct of research.

Received: October 28, 2022
Revised: December 16, 2022
Accepted: January 26, 2023
Published: February 9, 2023

REFERENCES

1. Bolouri, H., Farrar, J.E., Triche, T., Ries, R.E., Lim, E.L., Alonzo, T.A., Ma, Y., Moore, R., Mungall, A.J., Marra, M.A., et al. (2018). The molecular landscape of pediatric acute myeloid leukemia reveals recurrent structural alterations and age-specific mutational interactions. Nat. Med. *24*, 103–112. https://doi.org/10.1038/nm.4439.
2. Bowman, R.L., Busque, L., and Levine, R.L. (2018). Clonal hematopoiesis and evolution to hematopoietic malignancies. Cell Stem Cell *22*, 157–170. https://doi.org/10.1016/j.stem.2018.01.011.
3. Krivtsov, A.V., and Armstrong, S.A. (2007). MLL translocations, histone modifications and leukaemia stem-cell development. Nat. Rev. Cancer *7*, 823–833. https://doi.org/10.1038/nrc2253.
4. Brown, P. (2013). Treatment of infant leukemias: challenge and promise. Hematology. Am. Soc. Hematol. Educ. Program *2013*, 596–600. https://doi.org/10.1182/asheducation-2013.1.596.
5. Chaudhury, S.S., Morison, J.K., Gibson, B.E.S., and Keeshan, K. (2015). Insights into cell ontogeny, age, and acute myeloid leukemia. Exp. Hematol. *43*, 745–755. https://doi.org/10.1016/j.exphem.2015.05.008.
6. Chung, S.S., and Park, C.Y. (2017). Aging, hematopoiesis, and the myelodysplastic syndromes. Blood Adv. *1*, 2572–2578. https://doi.org/10.1182/bloodadvances.2017009852.
7. Gale, K.B., Ford, A.M., Repp, R., Borkhardt, A., Keller, C., Eden, O.B., and Greaves, M.F. (1997). Backtracking leukemia to birth: identification of clonotypic gene fusion sequences in neonatal blood spots. Proc. Natl. Acad. Sci. USA *94*, 13950–13954. https://doi.org/10.1073/pnas.94.25.13950.
8. Jones, L.K., Neat, M.J., van Delft, F.W., Mitchell, M.P., Adamaki, M., Stoneham, S.J., Patel, N., and Saha, V. (2003). Cryptic rearrangement involving MLL and AF10 occurring in utero. Leukemia *17*, 1667–1669. https://doi.org/10.1038/sj.leu.2403039.
9. Vishnu Tewari, V., Mehta, R., and Tewari, K. (2017). Congenital acute leukemia: a rare hematological malignancy. J. Neonatal Biol. *06*. https://doi.org/10.4172/2167-0897.1000265.
10. Cazzola, A., Cazzaniga, G., Biondi, A., Meneveri, R., Brunelli, S., and Azzoni, E. (2020). Prenatal origin of pediatric leukemia: lessons from hematopoietic development. Front. Cell Dev. Biol. *8*, 618164. https://doi.org/10.3389/fcell.2020.618164.
11. Yuan, J., Nguyen, C.K., Liu, X., Kanellopoulou, C., and Muljo, S.A. (2012). Lin28b reprograms adult bone marrow hematopoietic progenitors to mediate fetal-like lymphopoiesis. Science *335*, 1195–1200. https://doi.org/10.1126/science.1216557.
12. Copley, M.R., Babovic, S., Benz, C., Knapp, D.J.H.F., Beer, P.A., Kent, D.G., Wohrer, S., Treloar, D.Q., Day, C., Rowe, K., et al. (2013). The Lin28b–let-7–Hmga2 axis determines the higher self-renewal potential of fetal haematopoietic stem cells. Nat. Cell Biol. *15*, 916–925. https://doi.org/10.1038/ncb2783.
13. Viswanathan, S.R., Daley, G.Q., and Gregory, R.I. (2008). Selective blockade of MicroRNA processing by Lin28. Science *320*, 97–100. https://doi.org/10.1126/science.1154040.
14. Zhou, Y., Li, Y.-S., Bandi, S.R., Tang, L., Shinton, S.A., Hayakawa, K., and Hardy, R.R. (2015). Lin28b promotes fetal B lymphopoiesis through the transcription factor Arid3a. J. Exp. Med. *212*, 569–580. https://doi.org/10.1084/jem.20141510.
15. Manier, S., Powers, J.T., Sacco, A., Glavey, S.V., Huynh, D., Reagan, M.R., Salem, K.Z., Moschetta, M., Shi, J., Mishima, Y., et al. (2017). The

LIN28B/let-7 axis is a novel therapeutic pathway in multiple myeloma. Leukemia *31*, 853–860. https://doi.org/10.1038/leu.2016.296.

16. Wilbert, M.L., Huelga, S.C., Kapeli, K., Stark, T.J., Liang, T.Y., Chen, S.X., Yan, B.Y., Nathanson, J.L., Hutt, K.R., Lovci, M.T., et al. (2012). LIN28 binds messenger RNAs at GGAGA motifs and regulates splicing factor abundance. Mol. Cell *48*, 195–206. https://doi.org/10.1016/j.molcel.2012.08.004.
17. Hafner, M., Max, K.E.A., Bandaru, P., Morozov, P., Gerstberger, S., Brown, M., Molina, H., and Tuschl, T. (2013). Identification of mRNAs bound and regulated by human LIN28 proteins and molecular requirements for RNA recognition. RNA *19*, 613–626. https://doi.org/10.1261/rna.036491.112.
18. Wang, S., Chim, B., Su, Y., Khil, P., Wong, M., Wang, X., Foroushani, A., Smith, P.T., Liu, X., Li, R., et al. (2019). Enhancement of LIN28B-induced hematopoietic reprogramming by IGF2BP3. Genes Dev. *33*, 1048–1068. https://doi.org/10.1101/gad.325100.119.
19. Basak, A., Munschauer, M., Lareau, C.A., Montbleau, K.E., Ulirsch, J.C., Hartigan, C.R., Schenone, M., Lian, J., Wang, Y., Huang, Y., et al. (2020). Control of human hemoglobin switching by LIN28B-mediated regulation of BCL11A translation. Nat. Genet. *52*, 138–145. https://doi.org/10.1038/s41588-019-0568-7.
20. Balzeau, J., Menezes, M.R., Cao, S., and Hagan, J.P. (2017). The LIN28/let-7 pathway in cancer. Front. Genet. *8*, 31. https://doi.org/10.3389/fgene.2017.00031.
21. Jiang, X., Huang, H., Li, Z., Li, Y., Wang, X., Gurbuxani, S., Chen, P., He, C., You, D., Zhang, S., et al. (2012). Blockade of miR-150 maturation by MLL-fusion/MYC/LIN-28 is required for MLL-associated leukemia. Cancer Cell *22*, 524–535. https://doi.org/10.1016/j.ccr.2012.08.028.
22. Chen, L., Sun, Y., Wang, J., Jiang, H., and Muntean, A.G. (2016). Differential regulation of the c-Myc/Lin28 axis discriminates subclasses of rearranged MLL leukemia. Oncotarget *7*, 25208–25223. https://doi.org/10.18632/oncotarget.8199.
23. Zhou, J., Bi, C., Ching, Y.Q., Chooi, J.-Y., Lu, X., Quah, J.Y., Toh, S.H.-M., Chan, Z.-L., Tan, T.Z., Chong, P.S., and Chng, W.J. (2017). Inhibition of LIN28B impairs leukemia cell growth and metabolism in acute myeloid leukemia. J. Hematol. Oncol. *10*, 138. https://doi.org/10.1186/s13045-017-0507-y.
24. De Luca, L., Trino, S., Laurenzana, I., Tagliaferri, D., Falco, G., Grieco, V., Bianchino, G., Nozza, F., Campia, V., D'Alessio, F., et al. (2017). Knockdown of miR-128a induces Lin28a expression and reverts myeloid differentiation blockage in acute myeloid leukemia. Cell Death Dis. *8*, e2849. https://doi.org/10.1038/cddis.2017.253.
25. Okeyo-Owuor, T., Li, Y., Patel, R.M., Yang, W., Casey, E.B., Cluster, A.S., Porter, S.N., Bryder, D., and Magee, J.A. (2019). The efficiency of murine MLL-ENL-driven leukemia initiation changes with age and peaks during neonatal development. Blood Adv. *3*, 2388–2399. https://doi.org/10.1182/bloodadvances.2019000554.
26. GenomeOC. (2013). Therapeutically Applicable Research to Generate Effective Treatments (Office of Cancer Genomics). https://ocg.cancer.gov/programs/target.
27. Tyner, J.W., Tognon, C.E., Bottomly, D., Wilmot, B., Kurtz, S.E., Savage, S.L., Long, N., Schultz, A.R., Traer, E., Abel, M., et al. (2018). Functional genomic landscape of acute myeloid leukaemia. Nature *562*, 526–531. https://doi.org/10.1038/s41586-018-0623-z.
28. Lavallée, V.P., Baccelli, I., Krosl, J., Wilhelm, B., Barabé, F., Gendron, P., Boucher, G., Lemieux, S., Marinier, A., Meloche, S., et al. (2015). The transcriptomic landscape and directed chemical interrogation of MLL-rearranged acute myeloid leukemias. Nat. Genet. *47*, 1030–1037. https://doi.org/10.1038/ng.3371.
29. Pabst, C., Bergeron, A., Lavallée, V.P., Yeh, J., Gendron, P., Norddahl, G.L., Krosl, J., Boivin, I., Deneault, E., Simard, J., et al. (2016). GPR56 identifies primary human acute myeloid leukemia cells with high repopulating potential in vivo. Blood *127*, 2018–2027, –2027. https://doi.org/10.1182/blood-2015-11-683649.
30. Lavallée, V.P., Lemieux, S., Boucher, G., Gendron, P., Boivin, I., Armstrong, R.N., Sauvageau, G., and Hébert, J. (2016). RNA-sequencing analysis of core binding factor AML identifies recurrent ZBTB7A mutations and defines RUNX1-CBFA2T3 fusion signature. Blood *127*, 2498–2501. https://doi.org/10.1182/blood-2016-03-703868.
31. Bottomly, D., Long, N., Schultz, A.R., Kurtz, S.E., Tognon, C.E., Johnson, K., Abel, M., Agarwal, A., Avaylon, S., Benton, E., et al. (2022). Integrative analysis of drug response and clinical outcome in acute myeloid leukemia. Cancer Cell *40*, 850–864.e9. https://doi.org/10.1016/j.ccell.2022.07.002.
32. Ugale, A., Norddahl, G.L., Wahlestedt, M., Säwén, P., Jaako, P., Pronk, C.J., Soneji, S., Cammenga, J., and Bryder, D. (2014). Hematopoietic stem cells are intrinsically protected against MLL-ENL-mediated transformation. Cell Rep. *9*, 1246–1255. https://doi.org/10.1016/j.celrep.2014.10.036.
33. Wallace, J.A., and O'Connell, R.M. (2017). MicroRNAs and acute myeloid leukemia: therapeutic implications and emerging concepts. Blood *130*, 1290–1301. https://doi.org/10.1182/blood-2016-10-697698.
34. Zhu, H., Shyh-Chang, N., Segrè, A.V., Shinoda, G., Shah, S.P., Einhorn, W.S., Takeuchi, A., Engreitz, J.M., Hagan, J.P., Kharas, M.G., et al. (2011). The Lin28/let-7 axis regulates glucose metabolism. Cell *147*, 81–94. https://doi.org/10.1016/j.cell.2011.08.033.
35. Yuan, O., Ugale, A., de Marchi, T., Anthonydhason, V., Konturek-Ciesla, A., Wan, H., Eldeeb, M., Drabe, C., Jassinskaja, M., Hansson, J., et al. (2022). A somatic mutation in moesin drives progression into acute myeloid leukemia. Sci. Adv. *8*, eabm9987. https://doi.org/10.1126/sciadv.abm9987.
36. Zuber, J., Radtke, I., Pardee, T.S., Zhao, Z., Rappaport, A.R., Luo, W., McCurrach, M.E., Yang, M.-M., Dolan, M.E., Kogan, S.C., et al. (2009). Mouse models of human AML accurately predict chemotherapy response. Genes Dev. *23*, 877–889. https://doi.org/10.1101/gad.1771409.
37. Mootha, V.K., Lindgren, C.M., Eriksson, K.-F., Subramanian, A., Sihag, S., Lehar, J., Puigserver, P., Carlsson, E., Ridderstråle, M., Laurila, E., et al. (2003). PGC-1α-responsive genes involved in oxidative phosphorylation are coordinately downregulated in human diabetes. Nat. Genet. *34*, 267–273. https://doi.org/10.1038/ng1180.
38. Subramanian, A., Tamayo, P., Mootha, V.K., Mukherjee, S., Ebert, B.L., Gillette, M.A., Paulovich, A., Pomeroy, S.L., Golub, T.R., Lander, E.S., and Mesirov, J.P. (2005). Gene set enrichment analysis: a knowledge-based approach for interpreting genome-wide expression profiles. Proc. Natl. Acad. Sci. USA *102*, 15545–15550. https://doi.org/10.1073/pnas.0506580102.
39. Ross, M.E., Mahfouz, R., Onciu, M., Liu, H.-C., Zhou, X., Song, G., Shurtleff, S.A., Pounds, S., Cheng, C., Ma, J., et al. (2004). Gene expression profiling of pediatric acute myelogenous leukemia. Blood *104*, 3679–3687. https://doi.org/10.1182/blood-2004-03-1154.
40. Mullighan, C.G., Kennedy, A., Zhou, X., Radtke, I., Phillips, L.A., Shurtleff, S.A., and Downing, J.R. (2007). Pediatric acute myeloid leukemia with NPM1 mutations is characterized by a gene expression profile with dysregulated HOX gene expression distinct from MLL-rearranged leukemias. Leukemia *21*, 2000–2009. https://doi.org/10.1038/sj.leu.2404808.
41. Ng, S.W.K., Mitchell, A., Kennedy, J.A., Chen, W.C., McLeod, J., Ibrahimova, N., Arruda, A., Popescu, A., Gupta, V., Schimmer, A.D., et al. (2016). A 17-gene stemness score for rapid determination of risk in acute leukaemia. Nature *540*, 433–437. https://doi.org/10.1038/nature20598.
42. Liberzon, A., Birger, C., Thorvaldsdóttir, H., Ghandi, M., Mesirov, J.P., and Tamayo, P. (2015). The molecular signatures database hallmark gene set collection. Cell Syst. *1*, 417–425. https://doi.org/10.1016/j.cels.2015.12.004.
43. Cao, J., O'Day, D.R., Pliner, H.A., Kingsley, P.D., Deng, M., Daza, R.M., Zager, M.A., Aldinger, K.A., Blecher-Gonen, R., Zhang, F., et al. (2020). A human cell atlas of fetal gene expression. Science *370*, eaba7721. https://doi.org/10.1126/science.aba7721.
44. Zuber, J., Rappaport, A.R., Luo, W., Wang, E., Chen, C., Vaseva, A.V., Shi, J., Weissmueller, S., Fellmann, C., Taylor, M.J., et al. (2011). An integrated approach to dissecting oncogene addiction implicates a Myb-coordinated

self-renewal program as essential for leukemia maintenance. Genes Dev. *25*, 1628–1640. https://doi.org/10.1101/gad.17269211.

45. Petri, R., Pircs, K., Jönsson, M.E., Åkerblom, M., Brattås, P.L., Klussendorf, T., and Jakobsson, J. (2017). let-7 regulates radial migration of new-born neurons through positive regulation of autophagy. EMBO J. *36*, 1379–1391. https://doi.org/10.15252/embj.201695235.
46. Huppertz, I., Attig, J., D'Ambrogio, A., Easton, L.E., Sibley, C.R., Sugimoto, Y., Tajnik, M., König, J., and Ule, J. (2014). iCLIP: protein–RNA interactions at nucleotide resolution. Methods *65*, 274–287. https://doi.org/10.1016/j.ymeth.2013.10.011.
47. Tavner, F.J., Simpson, R., Tashiro, S., Favier, D., Jenkins, N.A., Gilbert, D.J., Copeland, N.G., Macmillan, E.M., Lutwyche, J., Keough, R.A., et al. (1998). Molecular cloning reveals that the p160 myb-binding protein is a novel, predominantly nucleolar protein which may play a role in transactivation by myb. Mol. Cell Biol. *18*, 989–1002. https://doi.org/10.1128/MCB.18.2.989.
48. Felipe-Abrio, B., Verdugo-Sivianes, E.M., Sáez, C., and Carnero, A. (2019). Loss of MYBBP1A induces cancer stem cell activity in renal cancer. Cancers *11*, 235. https://doi.org/10.3390/cancers11020235.
49. Mori, S., Bernardi, R., Laurent, A., Resnati, M., Crippa, A., Gabrieli, A., Keough, R., Gonda, T.J., and Blasi, F. (2012). Myb-binding protein 1A (MYBBP1A) is essential for early embryonic development, controls cell cycle and mitosis, and acts as a tumor suppressor. PLoS One *7*, e39723. https://doi.org/10.1371/journal.pone.0039723.
50. Jassinskaja, M., Pimková, K., Arh, N., Johansson, E., Davoudi, M., Pereira, C.-F., Sitnicka, E., and Hansson, J. (2021). Ontogenic shifts in cellular fate are linked to proteotype changes in lineage-biased hematopoietic progenitor cells. Cell Rep. *34*, 108894. https://doi.org/10.1016/j.celrep.2021.108894.
51. Lai, Y., Qiao, M., Song, M., Weintraub, S.T., and Shiio, Y. (2011). Quantitative proteomics identifies the myb-binding protein p160 as a novel target of the von Hippel-lindau tumor suppressor. PLoS One *6*, e16975. https://doi.org/10.1371/journal.pone.0016975.
52. Bellon, T., Perrotti, D., and Calabretta, B. (1997). Granulocytic differentiation of normal hematopoietic precursor cells induced by transcription factor PU.1 correlates with negative regulation of the c-myb promoter. Blood *90*, 1828–1839. https://doi.org/10.1182/blood.V90.5.1828.
53. Kim, S., Kim, D., Cho, S.W., Kim, J., and Kim, J.-S. (2014). Highly efficient RNA-guided genome editing in human cells via delivery of purified Cas9 ribonucleoproteins. Genome Res. *24*, 1012–1019. https://doi.org/10.1101/gr.171322.113.
54. Gundry, M.C., Brunetti, L., Lin, A., Mayle, A.E., Kitano, A., Wagner, D., Hsu, J.I., Hoegenauer, K.A., Rooney, C.M., Goodell, M.A., and Nakada, D. (2016). Highly efficient genome editing of murine and human hematopoietic progenitor cells by CRISPR/Cas9. Cell Rep. *17*, 1453–1461. https://doi.org/10.1016/j.celrep.2016.09.092.
55. Basson, M.A. (2012). Signaling in cell differentiation and morphogenesis. Cold Spring Harb. Perspect. Biol. *4*, a008151. https://doi.org/10.1101/cshperspect.a008151.
56. Filbin, M., and Monje, M. (2019). Developmental origins and emerging therapeutic opportunities for childhood cancer. Nat. Med. *25*, 367–376. https://doi.org/10.1038/s41591-019-0383-9.
57. Ramaswamy, K., Forbes, L., Minuesa, G., Gindin, T., Brown, F., Kharas, M.G., Krivtsov, A.V., Armstrong, S.A., Still, E., de Stanchina, E., et al. (2018). Peptidomimetic blockade of MYB in acute myeloid leukemia. Nat. Commun. *9*, 110. https://doi.org/10.1038/s41467-017-02618-6.
58. Velasco-Hernandez, T., Hyrenius-Wittsten, A., Rehn, M., Bryder, D., and Cammenga, J. (2014). HIF-1α can act as a tumor suppressor gene in murine acute myeloid leukemia. Blood *124*, 3597–3607. https://doi.org/10.1182/blood-2014-04-567065.
59. Dunwoodie, S.L. (2009). The role of hypoxia in development of the mammalian embryo. Dev. Cell *17*, 755–773. https://doi.org/10.1016/j.devcel.2009.11.008.
60. Felipe-Abrio, B., and Carnero, A. (2020). The tumor suppressor roles of MYBBP1A, a major contributor to metabolism plasticity and stemness. Cancers *12*, 254. https://doi.org/10.3390/cancers12010254.
61. de Beauchamp, L., Himonas, E., and Helgason, G.V. (2022). Mitochondrial metabolism as a potential therapeutic target in myeloid leukaemia. Leukemia *36*, 1–12. https://doi.org/10.1038/s41375-021-01416-w.
62. Balzer, E., and Moss, E.G. (2007). Localization of the developmental timing regulator Lin28 to mRNP complexes, P-bodies and stress granules. RNA Biol. *4*, 16–25. https://doi.org/10.4161/rna.4.1.4364.
63. Polesskaya, A., Cuvellier, S., Naguibneva, I., Duquet, A., Moss, E.G., and Harel-Bellan, A. (2007). Lin-28 binds IGF-2 mRNA and participates in skeletal myogenesis by increasing translation efficiency. Genes Dev. *21*, 1125–1138. https://doi.org/10.1101/gad.415007.
64. Jin, J., Jing, W., Lei, X.-X., Feng, C., Peng, S., Boris-Lawrie, K., and Huang, Y. (2011). Evidence that Lin28 stimulates translation by recruiting RNA helicase A to polysomes. Nucleic Acids Res. *39*, 3724–3734. https://doi.org/10.1093/nar/gkq1350.
65. Samsonova, A., El Hage, K., Desforges, B., Joshi, V., Clément, M.J., Lambert, G., Henrie, H., Babault, N., Craveur, P., Maroun, R.C., et al. (2021). Lin28, a major translation reprogramming factor, gains access to YB-1-packaged mRNA through its cold-shock domain. Commun. Biol. *4*, 359. https://doi.org/10.1038/s42003-021-01862-3.
66. Schneider, C.A., Rasband, W.S., and Eliceiri, K.W. (2012). NIH Image to ImageJ: 25 years of image analysis. Nat. Methods *9*, 671–675. https://doi.org/10.1038/nmeth.2089.
67. Pear, W.S., Miller, J.P., Xu, L., Pui, J.C., Soffer, B., Quackenbush, R.C., Pendergast, A.M., Bronson, R., Aster, J.C., Scott, M.L., and Baltimore, D. (1998). Efficient and rapid induction of a chronic myelogenous leukemia-like myeloproliferative disease in mice receiving P210 bcr/abl-Transduced bone marrow. Blood *92*, 3780–3792. https://doi.org/10.1182/blood.V92.10.3780.
68. Fan, M., Rhee, J., St-Pierre, J., Handschin, C., Puigserver, P., Lin, J., Jäeger, S., Erdjument-Bromage, H., Tempst, P., and Spiegelman, B.M. (2004). Suppression of mitochondrial respiration through recruitment of p160 myb binding protein to PGC-1α: modulation by p38 MAPK. Genes Dev. *18*, 278–289. https://doi.org/10.1101/gad.1152204.
69. Guzzi, N., Cieśla, M., Ngoc, P.C.T., Lang, S., Arora, S., Dimitriou, M., Pimková, K., Sommarin, M.N.E., Munita, R., Lubas, M., et al. (2018). Pseudouridylation of tRNA-derived fragments steers translational control in stem cells. Cell *173*, 1204–1216.e26. https://doi.org/10.1016/j.cell.2018.03.008.
70. Smith, T., Heger, A., and Sudbery, I. (2017). UMI-tools: modeling sequencing errors in Unique Molecular Identifiers to improve quantification accuracy. Genome Res. *27*, 491–499. https://doi.org/10.1101/gr.209601.116.
71. Dobin, A., Davis, C.A., Schlesinger, F., Drenkow, J., Zaleski, C., Jha, S., Batut, P., Chaisson, M., and Gingeras, T.R. (2013). STAR: ultrafast universal RNA-seq aligner. Bioinformatics *29*, 15–21. https://doi.org/10.1093/bioinformatics/bts635.
72. Uren, P.J., Bahrami-Samani, E., Burns, S.C., Qiao, M., Karginov, F.V., Hodges, E., Hannon, G.J., Sanford, J.R., Penalva, L.O.F., and Smith, A.D. (2012). Site identification in high-throughput RNA–protein interaction data. Bioinformatics *28*, 3013–3020. https://doi.org/10.1093/bioinformatics/bts569.
73. Bailey, T.L., Johnson, J., Grant, C.E., and Noble, W.S. (2015). The MEME suite. Nucleic Acids Res. *43*, W39–W49. https://doi.org/10.1093/nar/gkv416.
74. Norddahl, G.L., Pronk, C.J., Wahlestedt, M., Sten, G., Nygren, J.M., Ugale, A., Sigvardsson, M., and Bryder, D. (2011). Accumulating mitochondrial DNA mutations drive premature hematopoietic aging phenotypes distinct from physiological stem cell aging. Cell Stem Cell *8*, 499–510. https://doi.org/10.1016/j.stem.2011.03.009.

STAR★METHODS

KEY RESOURCES TABLE

REAGENT or RESOURCE	SOURCE	IDENTIFIER
Antibodies		
Anti-mouse CD117 (c-Kit)-APC	Biolegend	Cat# 105812, RRID: AB_313221
Anti-mouse/human B220 Biotin	Biolegend	Cat# 103203, RRID: AB_312988
Anti-mouse CD4-Biotin	SONY	Cat# 1102020, RRID: AB_1848918
Anti-mouse CD8-Biotin	SONY	Cat# 1103520, RRID: AB_962670
Anti -mouse Ly-6G/Ly-6C (Gr-1)-Biotin	Biolegend	Cat# 108404, RRID: AB_313369
Anti -mouse TER-119-Biotin	Biolegend	Cat# 116203, RRID: AB_313704
Anti -mouse Ly-6A/E (Sca-1)-Pacific Blue	Biolegend	Cat# 122520, Clone E13–161.7, RRID: AB_493274
Sav Brilliant Violet 605	SONY	Cat# 2626145
Anti -mouse CD48-FITC	Biolegend	Cat# 103404, RRID: AB_313018
Anti-mouse CD150-PE	Biolegend	Cat# 115904, RRID: AB_313683
Anti-mouse CD11b-APC	SONY	Cat# 1106060
Ly-6G-APC/Fire 750	BioLegend	Cat# 127652, RRID: AB_2616733
β-Actin	Cell Signaling Technology	Cat# 4970, RRID: AB_2223172
Anti- FLAG	Invitrogen	Cat# PA1-984B, RRID: AB_347227
MYBBP1A	Proteintech	Cat# 14524-1-AP, RRID: AB_2148137
Chemicals, peptides, and recombinant proteins		
Retronectin	Takara Bio	T100 A/B
Doxycycline Food 2 g/kg	Ssniff Spezialdiäten	A153D70623
Recombinant S. pyogenes Cas9 nuclease	Integrated DNA Technologies	1081059
Recombinant Murine IL-3	Peprotech	213-13
Recombinant Human Flt3-Ligand	Peprotech	300-19
Recombinant Murine SCF	Peprotech	250-03
Critical commercial assays		
Q5 Site-Directed Mutagenesis Kit	New England Biolabs	E0554S
Lipofectamine LTX Reagent with PLUS Reagent	Thermo Fisher	15338100
miRNeasy for Animal Cells	QIAGEN	217084
QIAseq miRNA Library Kit	QIAGEN	331502
TruSeq Stranded mRNA Library Prep	Illumina	20020594
Single Cell RNA Purification Kit	Norgen Biotek	51800
Magna RIP™ RNA-Binding Protein Immunoprecipitation Kit	Sigma-Aldrich	17-700
SuperScript III First-Strand Synthesis System	Invitrogen	18080051
SsoFast EvaGreen Supermix with Low ROX	Bio-Rad	172-5212
PureLink Genomic DNA Isolation Kit	Thermo Fisher	K182001
Q5 High-Fidelity DNA Polymerase	New England Biolabs	M0491S
Deposited data		
Raw and analyzed data	This paper	GEO: GSE201373
Experimental models: Cell lines		
THP-1	ATCC	RRID:CVCL_0006
Plat-E packaging cells	Cell_Biolabs	RRID: CVCL_B488
Phoenix-gp	ATCC	RRID:CVCL_H718

(*Continued on next page*)

Continued

REAGENT or RESOURCE	SOURCE	IDENTIFIER
Experimental models: Organisms/strains		
C57 BL/6N	Taconic	RRID: MGI:6196877
Homozygous iMLL-ENL (CD45.1)	Ugale et al.[32]	N/A
Heterozygous iLIN28B (CD45.2)	Zhu et al.[34]	N/A
Oligonucleotides		
See Table S5		
Recombinant DNA		
MigR1 plasmid	Addgene	RRID:Addgene_27490
Ms.HrasQ61L	This study	
pcDNA-p160MBP	Addgene	RRID:Addgene_41
Software and algorithms		
FlowJo™ v10.8 Software	BD Life Sciences	RRID:SCR_008520
GraphPad Prism Software	GraphPad	RRID:SCR_002798
ImageJ	Schneider et al.[66]	https://imagej.nih.gov/ij/
Inference of CRISPR Edits (ICE)	Synthego	https://icestage.synthego.com/#/
Gene Set Enrichment Analysis (GSEA) Software	Subramanian, Tamayo, et al.[38]	http://www.broad.mit.edu/gsea/; RRID:SCR_003199
CellRadar tool	Karlsson lab	https://karlssong.github.io/cellradar/

RESOURCE AVAILABILITY

Lead contact

Further information and requests for resources and reagents should be directed to and will be fulfilled by the lead contact, David Bryder (David.Bryder@med.lu.se).

Materials availability

This study did not generate new unique animals or reagents.

Data and code availability

- miR-seq and RNA-seq data have been deposited at GEO and are publicly available as of the date of publication. Accession number is listed in the key resources table.
- This paper does not report original code.
- Any additional information required to reanalyze the data reported in this paper is available from the lead contact upon request.

EXPERIMENTAL MODEL AND SUBJECT DETAILS

Mice

Homozygous iMLL-ENL (CD45.1) mice[32] were crossed to heterozygous iLIN28B (CD45.2) mice[34] to obtain ME or L28BME mice. 8–12 weeks old female C57 BL/6N mice were used as recipients (Taconic, RRID: MGI:6196877). ME and L28BME mice were used at 8–14 weeks of age. Mice were maintained in the animal facilities at the Biomedical Center of Lund University, and all animal experiments were performed with the approval of a local ethics committee.

Cell line

THP-1 cells, a human cell line of a one-year-old male with an MLL-AF9 fusion oncogene, were obtained from ATCC. Cells were cultured in RPMI 1640 (Thermo Fisher) containing l-glutamine and supplemented with 10% FBS and 100 IU/mL Penicillin.

Patient data

mRNA sequencing data of adult and pediatric AML patients (OHSU,[27] GDAC Firehose, and TARGET[26]) and their associated clinical information were obtained from the Cancer Genome Atlas (TCGA) database.

METHOD DETAILS

Development of ME AML from GMLPs

GMLPs were isolated from ME or L28BME mice (CD45.1+/CD45.2+) as described.[32] Briefly, BM cells were enriched using MACS magnetic enrichment for c-kit, followed by cell sorting (using FACS Aria II or III cell sorters, Becton Dickinson) and transplantation together with 300,000 unfractionated CD45.2 + BM cells into lethally irradiated (900 rad) CD45.2 + mice. Recipients were put on Doxycycline-containing diet 5 days prior to transplantation and throughout the whole experiment to ensure continuous expression of the transgene(s). Mortality, rapid elevations in donor myeloid chimerism, and signs of morbidity according to ethical guidelines were considered events for plotting event-free survival.

Retrovirus production and transduction

Hras cDNA was retrieved from a murine cDNA library and Gibson assembly (New England Biolabs) was used to clone the product into an EcoRI and XhoI linearized MigR1 retroviral vector.[67] A Q5 Site-Directed Mutagenesis Kit (New England Biolabs) was used to generate the HRAS Q61L GFP construct. MSN R295C mutant mCherry construct has been previously generated in our lab.[35] The pcDNA-p160MBP plasmid was a generous gift from Bruce Spiegelman (Addgene plasmid # 41 [68]) and was used to amplify the MYBBP1A cDNA, which was subsequently cloned into the MigR1 vector. The MYBBP1A P693A vector was generated using a Q5 Site-Directed Mutagenesis Kit (New England Biolabs) from the MigR1 MYBBP1A construct.

Replication incompetent retroviruses were produced by transfecting the vectors into Plat-E packaging cells (RRID: CVCL_B488) using Lipofectamine LTX Reagent with PLUS Reagent (Thermo Fisher). Virus-containing supernatants were harvested 48 h post transfection. Retroviral transductions were performed by centrifugation of the retrovirus (2 h, 1,200 g, 32°C) over Retronectin (Takara Bio) coated plates according to manufacturer's instructions and co-culture of GMLPs over the virus-coated wells for 48 h at 37°C.

GMLPs were cultured in StemSpan serum-free expansion media (Stem Cell Technologies) supplemented with 100 μM 2-Mercaptoethanol (Thermo Fisher), 5 ng/mL mIL3, 10 ng/mL hFlt3, 10 ng/mL mSCF (all from Peprotech) and 1 μg/mL doxycycline (Sigma-Aldrich).

Transplantation of transduced cells

48 h after transduction, GFP+ and/or mCherry + donor cells were sorted and competitively transplanted into lethally irradiated (900 rad) WT recipients together with 300,000 unfractionated WT BM cells per mouse. Recipients were put on a Doxycycline-containing diet 5 days prior to transplantation to ensure continuous expression of the transgene(s). Survival rates were plotted using the Kaplan-Meier method (GraphPad Prism). Mortality, rapid elevations in donor myeloid chimerism and signs of morbidity according to ethical guidelines were considered events for plotting event-free survival.

Serial replating assay

10,000 GMLPs were cultured in OPTI-MEM (Thermo Fisher) supplemented with 10% fetal bovine serum (FBS), 100 μM 2-Mercaptoethanol (Thermo Fisher), 5 ng/mL mIL3, 10 ng/mL hFlt3, 10 ng/mL mSCF (all from Peprotech) and 1 μg/mL doxycycline (Sigma-Aldrich). Cells were subjected to serial replating (1/10 of the well at each split) every third day. Cells were counted on day 12.

In vitro differentiation

Transduced cells were cultured under the previously mentioned conditions. Flow cytometry analysis was performed using CD11b-APC (SONY, Cat# 1106060) and Ly-6G-APC/Fire 750 (BioLegend, Cat# 127652) on BD LSRFortessa and LSRFortessa X-20 Cell Analyzers (Becton Dickinson).

Proteasomal inhibition

BM cells were isolated from ME or L28BME mice then Kit enrichment was performed. Cells were cultured for 4 days under the previously mentioned conditions with 1 μg/mL doxycycline (Sigma-Aldrich) to induce transgenes expression. After that, cells were treated with 10μM MG132 for 4h. Cells were then harvested, lysed, and WB was performed.

Western blotting

Cells were washed with ice-cold PBS then lysed in ice-cold RIPA lysis buffer (150 mM NaCl, 1% NP-40, 0.5% sodium-deoxycholate, 0.1% sodium dodecyl sulfate, 10 mM TrisHCl pH 8) supplemented with a protease inhibitor cocktail (Roche). Lysates were cleared by centrifugation at 15,000 rpm for 15 min at 4°C and supernatants were removed and assayed for protein concentration using the Quick Start Bradford Protein Assay Kit (Bio-Rad). Samples were denatured by mixing with appropriate amount of NuPAGE™ LDS Sample Buffer (4x) (Thermo Fisher) containing 2.5% 2-mercaptoethanol and heated to 95°C for 5 min. Equal amounts of proteins were loaded on an SDS-PAGE and transferred to PVDF membranes (Bio-Rad). Antibodies used were: mouse β-Actin (1:1,000, Cell Signaling Technology, 4970, RRID: AB_2223172), FLAG (Invitrogen, PA1-984B, RRID: AB_347227). and MYBBP1A (Proteintech Cat# 14524-1-AP, RRID:AB_2148137). Image analysis and quantification was performed using ImageJ.[66]

miRNA sequencing

GMLPs were cultured for 3–4 days in OPTI-MEM (Thermo Fisher) supplemented with 10% fetal bovine serum (FBS), 100 μM 2-Mercaptoethanol (Thermo Fisher), 5 ng/mL mIL3, 10 ng/mL hFlt3, 10 ng/mL mSCF (all from Peprotech) and 1 μg/mL doxycycline (Sigma-Aldrich). miRNA/small non-coding RNA sequencing was performed by QIAGEN. Briefly, RNA was isolated from $1x10^7$ cells using the miRNeasy for Animal Cells (QIAGEN) according to manufacturer's instructions. Library preparation was done using the QIAseq miRNA Library Kit (QIAGEN). A total of 500ng total RNA was converted into miRNA NGS libraries. Adapters containing UMIs were ligated to the RNA. RNA was converted to cDNA. The cDNA was amplified using PCR (13 cycles) and during the PCR indices were added. After PCR the samples were purified. Library preparation QC was performed. Libraries were pooled in equimolar ratios then sequenced on a NextSeq550 sequencing instrument according to the manufacturer instructions. Raw data was demultiplexed and FASTQ files for each sample were generated using the bcl2fastq software (Illumina inc.). Analysis was carried out using CLC Genomics Workbench (version 20.0.2) and CLC Genomics Server (version 20.0.2). Data has been deposited under the accession number GSE201373.

mRNA sequencing

GMLPs were cultured for 72 h then total RNA was isolated using the Single Cell RNA Purification Kit (Norgen Biotek). Library preparation was performed using TruSeq Stranded mRNA Library Prep (20020594, Illumina). Sequencing was performed on NovaSeq 6000 System (20012850, Illumina). Demultiplexing was performed using the bcl2fastq2 software. Read Mapping was performed using the HISAT2 software, and the reference genome sequence was from the Ensemble database, the Mouse GRCm38. Quantification of the expression levels of each gene was carried out using StringTie. Differentially expressed genes (DEG) analysis was performed using DESeq2. Data has been deposited under the accession number GSE201373.

iCLIP

iCLIP was performed as previously described with some modifications.[69] GMLPs isolated from L28BME (or ME as control for nonspecific binding) were expanded *in vitro*, 80 million cells per replicate were UV-crosslinked at 254 nm, with 200 mJ/cm^2 using UV Stratalinker 1800 (Stratagene) and pellets were snap frozen. Cells were harvested and lysed in iCLIP lysis buffer: 50 mM Tris/HCl pH 7.4, 100 mM NaCl, 0.5% Triton X-100, 0.5% sodium deoxycholate, 0.1% SDS, 5 mM EDTA and protease inhibitors (Sigma). Lysates were sonicated 4 × 10 s at 25 W using a Branson sonicator. Cell extracts were treated with 5 U/mL RNase I (Thermo Fisher) and 1 U/mL TURBO DNase (Thermo Fisher) for 3 min at 37°C with shaking at 1100 rpm. Lysates were kept on ice for 5 min and centrifuged at 15000 rpm for 10 min at 4°C. Supernatants were incubated with pre-washed anti-FLAG magnetic beads (Sigma) (40 μL per replicate) for 2 h at 4°C on rotator. Samples were washed with lysis buffer and incubated on-beads with 10 U/mL RNase I for 5 min at 37°C with constant shaking 1100 rpm. Reactions were blocked adding 1 mL of high salt (HS) buffer: 50 mM Tris/HCl, 1000 mM NaCl, 0.5% Triton X-100, 0.25% sodium deoxycholate, 1 M Urea, 5 mM EDTA, 1 mM DTT). Each sample was washed twice with HS buffer at 4°C, once with PNK/Tween buffer (20 mM Tris/HCl pH 7.4, 10 mM MgCl2, 0.2% Tween 20) and once with wash buffer (50 mM Tris/HCl pH 7.4, 10 mM MgCl2). Subsequently, samples were resuspended in 20 μL PNK dephosphorylation mix (4 μL 5X PNK buffer pH 6.5 (350 mM Tris-HCl pH 6.5, 50 mM MgCl2, 5 mM DTT), 0.5 μL T4 PNK (NEB), 0.5 μL SUPERase-IN RNase Inhibitor (Thermo Fisher) and incubated 15 min at 37°C. Samples were washed once with HS buffer, twice with wash buffer then resuspended in 20 μL of L3 adaptor ligation mix (2 μL 10X T4 RNA ligation mix (NEB), 1 μL T4 RNA ligase I (NEB), 0.5 μL SUPERase-IN RNase Inhibitor (Thermo Fisher), 1.5 pmol pre-adenylated L3 linker, 4 μL PEG400) and incubated shaking overnight at 16°C. Next, samples were washed twice with HS buffer, wash buffer and subsequently radiolabeled in 20 μL of T4 PNK mix containing 2 μL of 10X T4 PNK Buffer (NEB), 1 μL T4 PNK (NEB), 0.5 μL fresh γ-32P-ATP (PerkinElmer). Reactions were incubated 5 min at 37°C shaking at 1100 rpm and further washed once in HS and twice in PNK/Tween buffers. Beads were resuspended in 20 μL of 1.5 × Nu-PAGE loading buffer (Thermo Fisher) and incubated 10 min at 70°C, 1100 rpm. Supernatant was added to 1 μL 1 M DTT and boiled 3 min at 95°C. Samples were run on a NuPAGE 4%–12% Bis-Tris gel (Thermo Fisher) and transferred to a nitrocellulose membrane 0.45 μm (GE Healthcare). The remaining iCLIP library preparation steps were performed as previously described 6. Briefly, membranes containing protein-RNA complexes were excised and incubated in PK buffer at 37°C for 30 min with constant shaking at 1100 rpm. Reactions were terminated with an equal amount of PK buffer supplemented with 7 M urea. RNA was extracted using Phase Lock Gel Heavy tube (VWR) and ethanol-precipitated. cDNA synthesis was performed using using Superscript III (Thermo Fisher). cDNA was circularized using CircLigase II in the presence of 1M Betaine (Epicenter), annealed with 0.25 μM Cut oligo and digested with BamHI (Thermo Fisher). Digested cDNA was ethanol-precipitated and resuspended in 21 μL of water. 1 μL of cDNA was used for PCR amplification using HF Phusion (Thermo Fisher) with 18–21 PCR cycles. Libraries were sequenced on an Illumina MiSeq machine, with single-end for 50 cycles using MiSeq Reagent Kit v2 (50-cycles) (Illumina).

iCLIP-seq data analysis

Totally, ~23 million reads were obtained for read processing. The reads were classified into samples according to sample-specific barcodes. The barcodes and UMIs, 5 nucleotide unique sequence identifiers introduced during RT step, were removed and appended to the read name using UMI-tools.[70] The sequences were trimmed the 3′ adaptor sequence (AGATCGGAAG AGCGGTTCAG) by cutadapt v2.9 with parameter -m set to 18 and mapped to mouse genome mm10 using STAR v2.5.2b[71] with the following parameters: –outFilterMismatchNoverReadLmax 0.04 –outFilterMismatchNmax 999 –outFilterMultimapNmax 1 (unique mapping) or –outFilterMultimapNmax 100 (multiple mapping). PCR duplicates were removed based on UMIs using

UMI-tools. Peak identification was performed using Piranha v1.2.1[72] and motif analysis was performed using the MEME.[73] Peaks were annotated using Gencode vM25, miRBase and GtRNAdb2. Data has been deposited under the accession number GSE201083.

RIP-qPCR

RIP was performed on *in vitro* induced GMLPs using Magna RIP™ RNA-Binding Protein Immunoprecipitation Kit (Sigma-Aldrich). Approximately 2.0×10^7 cells were harvested, washed, and resuspended in complete RIP lysis buffer. Magnetic beads were washed and incubated with FLAG antibody or control normal rabbit IgG. Using magnetic separator, supernatant was discarded, and beads were washed. Magnetic beads were resuspended in RIP immunoprecipitation buffer and cell lysates were added to this mix. 10% of the cell lysate were kept aside as an input RNA sample for RT-PCR. The cell lysate-magnetic beads mix was incubated overnight at 4°C. Supernatant was discarded and beads were washed with cold RIP Wash Buffer. Both input sample and immunoprecipitates were treated with proteinase K buffer to digest the protein. Subsequently, supernatant was collected and washed with RIP Wash Buffer. RNA purification was performed using phenol:chloroform:isoamyl alcohol followed by overnight and ethanol precipitation. cDNA synthesis was carried out using SuperScript III First-Strand Synthesis System (Invitrogen).

Quantitative reverse-transcription PCR

Quantitative RT-PCR was performed as previously described.[74] Briefly, total RNA was isolated using a Single Cell RNA Purification Kit (Norgen Biotek) and converted to cDNA using SuperScript III First-Strand Synthesis System (Invitrogen). qRT-PCR reactions were run with SYBR GreenER (Invitrogen) on a CFX96 Touch Real-Time PCR Detection System (Bio-Rad). All signals were quantified using the ΔCt method and were normalized to β-actin mRNA expression levels.

THP-1 transduction

Phoenix-gp cell line was used to generate amphotropic MYBBP1A A693 retrovirus. Successfully transduced THP-1 cells were sorted, maintained in culture, and counted at the indicated timepoints.

CRISPR-Cas9 deletion of Mybbp1a

1 μL of the recombinant S. pyogenes Cas9 nuclease (1 μg/uL) (IDT) was mixed with three gRNAs targeting Mybbp1a (Synthego) at a final molar ratio of 1:6. The mix was incubated for 10 min at room temperature to allow for RNP complex formation. GMLPs from L28BME, which had been previously transduced with a retrovirus carrying the HRAS Q61L GFP construct, were resuspended in T-buffer for Neon electroporation (Thermo Fisher). The optimized Neon electroporation conditions were 1600 V, 20 ms, and one pulse for the 10 μL tip. For the control group, cells were mixed with a Cas9 nuclease that lacked any gRNA and were electroplated using the same conditions.

Mybbp1a gRNA sequences:
UCGCAGGCUCAGCUUUCGUG.
ACUCGCGGCUGUGCUCCAGC.
CGGAGCCGCGUUUCCUGAUC.

Genomic DNA isolation and analysis of knockout efficiency

gDNA was purified from electroporated cells using the PureLink Genomic DNA Isolation Kit (Thermo Fisher Scientific) and the edited region of Mybbp1a was amplified using Q5 High-Fidelity DNA Polymerase (New England Biolabs) with the following cycling conditions: 30 s at 98°C, 32 cycles of 10 s at 98°C, 30 s at 65°C, and 30 s at 72°C, followed by a final 2-min extension at 72°C. Primers used were CCCACAGCCACAAGGGAAA (forward) and CGAATCCTACGGAACCAAGAAC (reverse). Following PCR, Sanger sequencing of the barcodes was performed (Eurofins) using CCACAAGGGAAAGGCAAGGC as a sequencing primer. Finally, generated sequences were analyzed using the Inference of CRISPR Edits (ICE) online tool (Synthego) (https://icestage.synthego.com/#/) to determine the efficiency of Mybbp1a editing.

QUANTIFICATION AND STATISTICAL ANALYSIS

Data analysis was performed using GraphPad Prism (GraphPad Software) and Microsoft Excel. All FACS data were analyzed with FlowJo. Significance values were calculated by Student's two-tailed t test, ordinary one-way ANOVA, or the log rank test (Mantel-Cox test) for Kaplan-Meier curves. Statistical details of experiments can be found in figure legends, including statistical tests used and exact value of n. Bars indicate mean values, and error bars represent SEM. *$p < 0.05$, **$p < 0.01$, ***$p < 0.001$; n.s., not significant.